DIRECTOR

COMMONWEALTH OF AUSTRALIA

DEPARTMENT OF NATIONAL DEVELOPMENT

BUREAU OF MINERAL RESOURCES GEOLOGY AND GEOPHYSICS

RECORDS:

1965/56

CLINOENSTATITE IN A VOLCANIC ROCK FROM THE CAPE VOGEL AREA, PAPUA.

by

W.B. Dallwitz, J.E. Thompson, and D.H. Green

CLINOENSTATITE IN A VOLCANIC ROCK FROM THE CAPE VOGEL AREA, PAPUA.

by

W.B. DALLWITZ[1], J.E. THOMPSON[1], AND D.H. GREEN[2]

1. Bureau of Mineral Resources, Geology, and Geophysics, Canberra.

2. Department of Geophysics and Geochemistry, Australian National University, Canberra.

ABSTRACT

A porphyritic volcanic rock from Cape Vogel, Papua, contains abundant phenocrysts of multiply twinned clinoenstatite with less common phenocrysts of orthopyroxene, set in a groundmass of pyroxene microlites, glass, and zeolites. The rock contains 54% SiO_2, 13-16% MgO, and 6-7% FeO, but only 7-8% Al_2O_3, 4.5-5.5% CaO, and 0.6 - 0.8% Na_2O. Microprobe analyses show that the clinoenstatite phenocrysts range from En_{92} to En_{87}, and have very low Al_2O_3 and extremely low CaO contents. Their composition differs consistently from that of the orthopyroxene phenocrysts which range from En_{87} to at least as Fe-rich as En_{78}. The clinoenstatite phenocrysts are a metastable inversion product from primary protoenstatite. The crystallization of protoenstatite as the liquidus phase in this magma is attributed directly to the unique magma composition. The occurrence of this rock in a region of structural complexity between stable oceanic and continental crustal elements may have implications in terms of deep-crustal or upper-mantle petrogenetic processes.

INTRODUCTION

In the course of reconnaissance geological mapping on Cape Vogel in north-eastern Papua in 1954, J.E. Thompson collected two specimens of a dark grey, porphyritic, glassy rock with white zeolitic amygdales. These were examined by W.B. Dallwitz who found that they contained abundant prismatic crystals of clinoenstatite up to 8 mm. long; other constituents were pyroxene microlites,

altered glass, unaltered glass, zeolites, bronzite phenocrysts, and traces of chrome spinel.

No rock of this kind had been recorded in the literature, and analysis of the specimens confirmed the high magnesia content expected from the abundance of clinoenstatite. The analyses have been published in a compilation of Australian rock analyses (Joplin, 1963, pp. 182 and 189).

In February, 1964, the two aforementioned authors brought to the notice of Professor C.E. Tilley hand specimens, thin sections, and chemical analyses of the clinoenstatite-bearing rocks. He supported the earlier identification of clinoenstatite, and at the same time noted vestigial structures indicative of the former presence of protoenstatite. The assistance of D.H. Green was sought to carry out electron microprobe analyses on the pyroxenes.

The Cape Vogel area was first examined geologically in 1914 by Evan R. Stanley, then Government Geologist for the Territory of Papua. In an unpublished report (Stanley, 1916) he recorded "grey-coloured volcanic rocks...., containing amygdules and spherules of zeolitic minerals and large idiomorphic crystals of hornblende" from the locality where the clinoenstatite-bearing rocks were subsequently collected. He did not examine these rocks in thin section, and the mineral he referred to as hornblende was probably clinoenstatite.

Experimental studies on $MgSiO_3$ composition by Foster (1951), Atlas (1952), and Boyd and Schairer (1964) have extended the work of

earlier investigators, and clarified the relationships of the $MgSiO_3$ polymorphs. Orthoenstatite, the common natural polymorph, inverts to protoenstatite at high temperatures (above 985°C at atmospheric pressure). Clinoenstatite, monoclinic and usually polysynthetically twinned, may form as a metastable inversion product when protoenstatite is cooled through the protoenstatite-orthoenstatite inversion. Clinoenstatite occurs naturally in stony meteorites, but is extremely rare in terrestrial rocks. Members of the clinoenstatite-clinoferrosilite solid solution series have recently been identified as exsolution lamellae in an igneous and a metamorphic pyroxene (Binns, Long, and Reed, 1963).

LOCALITY (J.E.T., W.B.D.)

Cape Vogel is an easterly-aligned peninsula on the north-eastern coast of Papua (Fig.1). It is about 20 miles long and 10 to 15 miles wide, and is intricately dissected to a maximum relief of about 1,000 feet above sea level by a finely dendritic stream system.

The two specimens of clinoenstatite-rich rock were collected from exposures about half a mile apart near the former village site of Boboni on Dabi Creek, about three miles south-west of the mouth of this stream on the northern coastline between Tapio Bay and Magabara (Fig.2). The locality is about two and a half miles west-south-west of Castle Hill, a limestone prominence about 1,000 feet above sea level. Easiest access to the area is by foot

from Tapio Bay, where there is a shallow anchorage, a village, and a Government rest house. There is a small wharf suitable for coastal launches at Magabara, about three miles west of the mouth of Dabi Creek, and an airstrip suitable for light aircraft at Tarakururu Mission.

The area of outcrop from which the two specimens were taken is roughly oval, and is about 5,000 feet long, north-west to south-east, and 3,000 feet wide (Fig.2). Dabi Creek flows around the southern and eastern margin of this small area, which has low relief, is only slightly dissected and almost treeless, and supports a relatively thin cover of kangaroo grass (Themeda australis). The surrounding, higher, more intricately dissected hills of bedded Miocene and Pliocene clastic sediments and basic igneous rocks support many more trees, especially in gullies and near streams; the non-wooded and lightly wooded parts are characterized by a thick cover of kunai grass (Imperata cylindrica var. major). ~~The contrast is obvious on aerial photographs.~~

REGIONAL GEOLOGICAL ENVIRONMENT (J.E.T.)

Between longitudes 147° 00'E and 149° 30'E, Papua has a mountainous core consisting of folded and faulted (?)Palaeozoic schists, phyllites, and lenses of marble. At its north-western end, this metamorphic province has an arcuate trend - the Macroberie Arc (Glaessner, 1950) - and is intruded by granodiorite bodies of batholithic dimensions. Near 149° 00'E longitude, the metamorphic

rocks appear to have been offset some 30 miles to the north-north-east by left-lateral, strike-slip displacement along a topographically conspicuous, recently active, major fault (Fig.1). The alignment of vents in a Pleistocene to Recent andesitic volcanic complex at Cape Nelson suggests a northerly extension of this fault beneath Recent alluvium.

Fig. 1 ->

The mountains east of 149° 30'E longitude are not composed of the greenschist facies metasediments which form the main range, but consist mainly of basic igneous rocks, comprising dolerite and basic submarine lavas, which are locally intruded by swarms of phonolitic and trachyandesitic dykes, and by granodiorite at Milne Bay and inland from Cape Frere. Little is known of the structure of this mountainous region, but dislocation of fold axes in Pliocene sediments west of Cape Vogel suggests post-Pliocene left-lateral, strike-slip displacement along a fault in the underlying basement consistent with displacement of the metamorphic province in the direction of the D'Entrecasteaux Islands. The geology of these islands and the islands of the Louisiade Archipelago as far east as Sudest (beyond the eastern limit of Fig. 1) is dominated by metasedimentary rocks and granodiorite which may represent a laterally displaced part of the metamorphic province of the mainland of eastern Papua. From evidence of transcurrent fault displacements in the D'Entrecasteaux Islands, Davies and Ives (1965) have also postulated large-scale transcurrent displacement of the metamorphic core from the mainland of Papua to the present position of the

D'Entrecasteaux Islands.

Over most of its exposed length of about 230 miles, the north-eastern front of the metamorphic core on the Papuan mainland is in abrupt fault contact with a belt of ultramafic and basic plutonic rocks overlain by basic submarine lavas (Thompson, 1957, and unpublished maps). This belt has been variously called the Papuan Ultrabasic Belt (Thompson, 1957; Dow and Davies, 1964), Papuan Ultramafic Belt (Green, 1961), the Papuan Basic and Ultrabasic Belt (Smith and Green, 1961), and the Papuan Basic Belt (Dow and Davies, 1961). On the south-west and south-east, the metamorphic province is flanked by gabbro, dolerite, basic submarine lavas, chert, argillite, and fine-grained limestone - a typical ophiolitic suite. The contact between metamorphic rocks and ophiolites on the south-west and south-east has not been seen.

The Owen Stanley Fault (Fig. 1), which separates the metamorphic core from the Papuan Basic Belt, is a profound crustal break with a broadly sinuous trace recognised for over 200 miles. The fault forming the north-eastern margin of the Gorupu Mountains is possibly a dislocated extension of the Owen Stanley Fault. Ample topographic evidence indicates that the youngest vertical displacement on the Owen Stanley Fault and its suggested easterly extension has been upwards on the south-west. Stream deflections at the north-western end of the fault indicate recent left-lateral strike-slip displacement of about three miles (Dow and Davies, 1964).

The surface trace of the fault plane suggests a moderate to steep dip to the north-east.

The Papuan Basic Belt was probably emplaced by reverse faulting in post-Cretaceous to Lower Miocene time. Recent upward displacement of the metamorphic core is attributed to isostatic re-adjustment consequent on the emplacement of the heavy rocks of the Papuan Basic Belt on top of lighter rocks of the metamorphic province.

The northern two-thirds of the Papuan Basic Belt consist of an inner non-feldspathic, ultramafic zone against the Owen Stanley Fault, and an outer feldspathic zone overlain by basic submarine lava and dolerite (Thompson, 1957; Dow and Davies, 1964). At the south-eastern end of the belt this simple zoning is not apparent (Smith and Green, 1961; Green, 1961). It has been suggested by Thompson, (in Dow and Davies, 1964) that the Papuan Basic Belt is actually a thick, north-easterly dipping slab of oceanic crust (cf. de Roever, 1957; Hess, 1960, 1964).

North of the faulted front of the Gorupu Mountains, Upper Miocene to Recent clastic sediments and Pleistocene to Recent volcanic products may conceal ultramafic and basic rocks co-extensive with those of the Papuan Basic Belt. Serpentinite boulders were ejected during the 1943-44 eruption of the Gorupu (Waiowa) volcano (Baker, 1946), and pebbles of basic igneous rocks are common constituents of late Tertiary conglomerates on Cape Vogel.

Lower Miocene limestones unconformable on probable sea-floor deposits of basic volcanic rocks have been recorded from the following three isolated localities in north-eastern Papua:

(1) near the intersection of 8°00S latitude and 148°00E longitude (Fig.1) (Crespin, Kicinski, Paterson, and Belford, 1956),

(2) at Castle Hill, Cape Vogel (Crespin and Belford, 1955), and

(3) at the base of the peninsula north of ~~on the northern arm of~~ Milne Bay (Belford, 1959).

An Upper Miocene succession of clastic sediments at least 14,000 feet thick (A.P.O.C., 1930) is exposed on Cape Vogel, and an unmeasured, but considerable, thickness (probably in excess of 5,000 feet) of poorly consolidated, moderately dipping conglomerates forms deeply dissected foothills along the coast between Goodenough Bay and Cape Frere. The sediments on Cape Vogel have been broadly folded and invaded by late Pliocene or Pleistocene basic intrusives and volcanics in a linear belt parallel to the north coast (Fig.2). The clinoenstatite-bearing rocks described in this paper occur near the eastern end of the intrusive/extrusive complex on Cape Vogel. Available field, palaeontological, and geochronological evidence indicates that they are pre-Lower Miocene (f 1-2 stage) submarine volcanics.

Recent vulcanism in north-eastern Papua has been

characteristically andesitic and explosive. The most recent activity began in 1951 when Mount Lamington erupted violently (Taylor, 1958). There are many older, eroded, volcanic vents in the Hydrographer Range, south-east of Mount Lamington; some of these produced basaltic lavas. The mountain block which forms Cape Nelson is an entirely andesitic volcanic complex; native legends suggest that vents in this area were last active about 1880. Just south of Cape Nelson, near the faulted front of the Gorupu Mountains, explosive andesitic eruptions began in late 1943, and continued through 1944 (Baker, 1946), in an area where no volcanic activity had previously been recorded.

LOCAL GEOLOGICAL ENVIRONMENT. (J.E.T.)

Cape Vogel peninsula is composed mainly of Upper Miocene and Pliocene calcareous siltstone, lithic sandstone, polymict conglomerate, and tuff, having an aggregate thickness in excess of 14,000 feet (A.P.O.C., 1930). This succession is broadly folded into an asymmetrical anticline having a roughly east-west axis parallel to, and about three miles inland from, the northern coastline (Fig.2). This fold has a gentle southern flank, with dips ranging from about 15° near the core to about 5° on the outer flank, and a steeper, poorly exposed, and structurally disturbed northern flank. No convincing lithological or palaeontological correlations have been made across the axis, and it is possible that the fold may be crestally faulted. Throughout the greater part of its length, the

axial zone of the fold is occupied by a belt of basaltic rocks from one half to one and a half miles wide. Sediments in contact with these basalts are usually silicified and indurated over distances ranging from a few feet to several hundred feet. Most of the available field evidence suggests that basaltic magma intruded and arched the thick sequence of sediments in late Pliocene time. It is also possible that the linear belt of basalt may merely be a young lava pile occupying an erosional valley along the crest of the anticline. However, the basaltic and doleritic rocks at the eastern end of the belt are unconformably overlain, at Castle Hill, by a limestone containing diagnostic Lower Miocene (f1-2 stage) larger foraminifera (Crespin and Belford, 1955, specimen LB109).

Fig. 2 →

The clinoenstatite-bearing specimens were collected during a single reconnaissance traverse across the small outcrop of igneous rocks west and north of Dabi Creek (Fig.2). This outcrop is overlain on the north-west by light brown Upper Miocene calcareous siltstone, and on the south by lithic sandstone; elsewhere the contact is concealed. Specimen LB 105 was collected within a few feet of the siltstone contact, and LB 107 came from near the centre of the outcrop area. The relationship of the clinoenstatite-bearing rock to the volcanics both to the east and the west could not be firmly established.

A specimen of glassy, unweathered clinoenstatite-bearing rock, collected when the area was re-visited in 1964, has been dated by Dr. I. McDougall, of the Department of Geophysics and Geochemistry, Australian National University, by K/Ar measurement on a whole-rock sample. He obtained a reliable minimum age of 28± 1 million years, which, according to the time-scale of Kulp (1961) corresponds to the top of the Oligocene. The sample dated is free from zeolites, but contains some small, brown, devitrified patches which amount to a few percent of the rock.

PETROGRAPHY. (W.B.D.)

In hand specimen, LB 107 is medium-grey to dark grey, and contains abundant euhedra of cloudy to lustrous, translucent, honey-coloured pyroxene, rarely up to 8 mm. long, in a groundmass consisting of glass crowded with acicular microlites, and containing scattered amygdales of a white zeolite up to 2 mm. across. Specimen LB 105 is generally similar to LB 107; it differs in being slightly darker, and in containing smaller and markedly fewer phenocrysts, many more, and somewhat larger, amygdales of zeolite, and numerous patches of greenish black, altered glass up to 0.5 mm. across; thin encrustations of aragonite may occur along some freshly broken faces.

The chemical analyses and C.I.P.W. norms of these rocks are given in Table 1.

Table 1 →

Noteworthy features of the rocks are the unusually high

TABLE 1

Chemical analyses and C.I.P.W. norms of clinoenstatite-bearing rocks.

	LB107	LB107 Water-free	LB105		C.I.P.W. Norms LB107	LB105
SiO_2	53.97	57.58	54.09	Qz	11.94	15.00
TiO_2	0.23	0.25	0.30	Or	2.22	2.22
Al_2O_3	7.08	7.55	8.39	Ab	5.24	6.27
Fe_2O_3	3.46	3.69	3.65	An	15.37	18.35
FeO	6.95	7.42	6.54	Wo	6.42	6.85
MnO	0.21	0.22	0.15	Hy	46.81	38.05
MgO	16.03	17.10	13.03	Il	0.45	0.61
CaO	4.79	5.11	5.46	Mt	5.10	5.33
Na_2O	0.60	0.64	0.75	H_2O+	6.07	7.36
K_2O	0.35	0.37	0.41	(P_2O_5)	0.06	0.07
P_2O_5	0.06	0.07	0.07			
Loss 110°C	1.73	-	2.70			
Loss 1000°C	4.34	-	4.66			
	99.80	100.00	100.20			
$\frac{Mg}{Mg + Fe^{++}}$ (mol)	80.5		78			
Normative pyroxene (mol. %)	$Wo_{7.4}En_{79.6}$ $Fs_{14.7}$		$Wo_{7.4}En_{78.0}$ $Fs_{14.6}$			

Analyst: A. McClure, 1960, formerly of Bureau of Mineral Resources, Geology, and Geophysics, Canberra.

water content, the low alumina and alkali contents, the high magnesia and iron oxide contents, relative to the silica percentage, and the lack of correspondence between the normative and modal compositions. The analyzed rocks are unweathered - the water is present in zeolites, altered glass, and possibly unaltered glass also. Their unusual composition becomes even more apparent when the analyses are re-calculated on a water-free basis: LB107 - SiO_2 58%, MgO 17%; LB105 - SiO_2 58%, MgO 14%.

In thin section, specimen LB107 is seen to consist of clinoenstatite and bronzite phenocrysts, abundant pyroxene microlites, lime-bearing, relatively iron-rich pyroxenes occurring as borders to the pyroxene phenocrysts and microlites, and also as individual microlites, altered and unaltered glass, zeolitic minerals, and traces of chrome spinel. Virtually all the ferric oxide must be in the glass, as the percentage of opaque mineral is very low. The general appearance of this rock is illustrated in Plate 1, fig. A.

The clinoenstatite phenocrysts are commonly euhedral, and are characterized by rather regularly spaced multiple twin-lamellae (Plate 1, figs. B and C) averaging about 0.015 mm. in width, and by a decidedly murky appearance, as compared with bronzite, in transmitted light. The murkiness is not due to alteration, but to closely spaced cracks, cleavages, and partings, and is accentuated, in the cores of some crystals, by abundant, minute, fluid and opaque inclusions. No exsolution lamellae are present. The lengths of the phenocrysts seen in three thin sections range

from 0.3 mm. to 3.6 mm., and their average size is about 1 mm.. Signs of a cleavage or parting perpendicular to the c-axis are visible, but individual cracks are rarely longer than about 0.02 mm.. An even more unusual feature is a pair of strong cleavages or partings (Plate 1, fig. D) almost invariably visible in sections cut parallel to the twin plane (100), and making ((?) apparent) angles of 64° with (010); such cleavages or partings are, as far as is known, quite distinct from any previously recorded in pyroxenes. The terminal faces of quite a few crystals are slightly concave (Plate 1, fig. D); an extreme example of curvature is illustrated in Plate 1, fig. C.

Most of the clinoenstatite crystals are bordered by a rim of green, calcic, iron-rich clinopyroxene about 0.01 mm. wide (Plate 1, fig. D); this rim and a straw-coloured or greenish yellow zone of similar width immediately inside of it have a birefringence greater than that of the clinoenstatite (Plate 2, fig. A). Wedge-shaped and acicular outgrowths of green pyroxene are developed on the terminal faces of some crystals (Plate 1, fig. D).

The bronzite phenocrysts in the sections examined range from 0.3 mm. to 2 mm. in length, and their average size is about 0.6 mm.. They are colourless, and are usually euhedral (Plate 1, fig. A; Plate 2, fig. B) or subhedral (Plate 2, figs. C and D). Two zones can commonly be seen between crossed nicols, but in one crystal (Plate 2, fig. B) four oscillatory zones are clearly visible (see also Table 5, No. 1). Some grains are partly mantled

by clinoenstatite (Plate 2, figs. C and D), and a few (Plate 2, figs. D and E) also contain inclusions of this mineral. Several aggregates of anhedral grains of bronzite were noted; one of those aggregates encloses a grain of clinoenstatite, and in another some probable exsolution lamellae of clinopyroxene were observed. Bronzite grains are commonly rimmed by green pyroxene similar to that surrounding clinoenstatite (Plate 2, fig. E), and wedge-shaped outgrowths of colourless and green pyroxene are usually developed on terminal faces. Some bronzite grains show cross-fractures at right angles to the c-axis (Plate 1, fig. A; Plate 2, fig. E; Plate 3, fig. D; Fig 3).

The microlites are acicular, and their average size is about 0.3 mm. x 0.035 mm. (Plate 3, fig. A). Little is known of their composition. Most consist of colourless pyroxene with low double refraction bordered by a thin zone of more highly birefringent colourless or yellowish green to green pyroxene which also occurs as feathery terminations on many crystals (Plate 3, figs. A and B), and as separate microlites. The general appearance of the colourless, rather weakly birefringent cores of many of the microlites is strongly suggestive of the clinoenstatite of the phenocrysts. Minute curved structures reminiscent of those found in clinoenstatite which has inverted from protoenstatite (C.E. Tilley, pers. comm.) are visible in some of them, but multiple twinning is rare, and is generally best seen in cross-sections. The twin lamellae are much thinner than those of the phenocrysts, and range from about 0.5 micron

to 5 microns in width. A few of the colourless cores are somewhat clearer than the majority, and are probably of bronzitic composition; however, it is mostly impossible to distinguish between microlites of orthopyroxene and sections of probable clinoenstatite cut approximately parallel to (100). It is possible that the cores of some microlites are untwinned clinoenstatite, as untwinned borders close to clinoenstatite composition were measured during electron microprobe analysis of some bronzite phenocrysts (Table 8, Nos. 2, 3). As the cores of many of the microlites have straight extinction, and yet are not as clear as the bronzite, it is also possible that some of them are protoenstatite which could have survived as a metastable phase.

The microlites have a very well developed parting or cleavage (Plate 3, figs. A and B) at right angles to their length. This feature was also mentioned in the description of the clinoenstatite and bronzite phenocrysts, but it is less prominent in these (especially the clinoenstatite) than in the microlites. Cross fractures with such an orientation seem not to have been previously described in pyroxenes.

In addition to the microlites already described there are much smaller greenish ones with curved, feathery shapes which make up about 1 percent of the rock.

Intermediate in size between the acicular microlites and the smallest phenocrysts (as arbitrarily designated here) are small

crystals of clinoenstatite and of bronzite and composite crystals of clinoenstatite and bronzite, some of which are illustrated in Pl. 2, fig. A, Plate 3, fig. C, and Fig. 3. The dimensions of such grains range from 0.07 mm. to 0.2 mm. in cross section, and up to 0.6 mm. in longitudinal section. The twin-lamellae in the clinoenstatite are thinner than those of the phenocrysts, and thicker than those of the microlites. Crystals of bronzite with slightly concave terminal faces coming to a sharp point are rather characteristic.

Fig. 3 →

The ratio of altered glass to unaltered glass shows a good deal of variation from one field of view to another. Where fresh, the glass is very pale greenish grey (almost colourless) and isotropic, and its refractive index is greater than that of Canada balsam. Where altered, the glass is light brown with a slight greenish tinge, and generally shows aggregate polarization on an extremely fine scale. In some places it forms very finely fibrous-radiating rims, about 0.002 mm. wide, around colourless zeolite or bodies of altered glass with aggregate polarization. The refractive index of the darker varieties of altered glass is appreciably less than that of balsam, whereas that of the less common lighter varieties - presumably in a less advanced stage of hydration - is slightly greater than that of balsam.

Five varieties of zeolite were distinguished in thin section, but none has, as yet, been identified. The sizes of the zeolite masses range down to about 0.1 mm. It appears that only

very few of the zeolite bodies fill pre-existing cavities, as their shapes are commonly quite irregular; most of them seem to have formed in the glass in the same way as do spherulites in acid volcanic rocks, and are generally indistinguishable from glass in hand specimen.

Except for a few larger grains, chrome spinel occurs almost entirely within phenocrysts of clinoenstatite and bronzite; its average grainsize is about 0.005 mm., but a few crystals range up to 0.4 mm. (Plate 1, fig. A). The smaller grains are dark red-brown in strong transmitted light.

Specimen LB105 is broadly similar to LB107, but shows differences in the percentages of some of the minerals, especially clinoenstatite phenocrysts and zeolites, and altered and unaltered glass. Its general appearance is illustrated in Plate 3, fig. D. In addition to the five zeolitic minerals noted in LB107, it contains a small quantity of a another (?)zeolite which is characterized by closely-spaced cleavage. A few veinlets of aragonite, about 1 micron thick, traverse the slide, and cross some of the larger masses of zeolite which appear to be normal vesicle fillings, and form the amygdales seen in hand specimen.

Micrometric analyses of specimens LB107 and LB105 are given in Table 2. Points were counted at 0.3 mm. centres. The distinction between phenocrysts and microlites was more difficult to make in LB105 than in LB107, and is, therefore, more arbitrary.

Table 2 →

TABLE 2

Micrometric analyses of clinoenstatite-bearing rocks.

	LB107 (4,145 points)		LB105 (3,146 points)	
Pyroxene				
Clinoenstatite phenocrysts	19		5	
Bronzite phenocrysts	2		1	
Colourless microlites (clino-enstatite, orthopyroxene, (?) protoenstatite, and calcic clinopyroxene, mostly composite crystals)	22		30	
Green and yellowish green to greenish yellow clinopyroxene:				
Bordering phenocrysts of clino-enstatite and bronzite	3)		1)	
Bordering colourless microlites, and as separate microlites	10)	14	10)	12
Feathery microlites	1)		1)	
Zeolites	8		12	
Unaltered glass	15)		6)	
Altered glass	20)	35	34)	40
Chromo spinel	<0.3		<0.3	
	100		100	

OPTICAL MEASUREMENTS ON THE PYROXENES. (W.B.D.)

Refractive index measurements on the clinoenstatite were confined to the larger phenocrysts. Grains chosen for measurement were those cut parallel to the twin plane (100) (Plate 1, fig. D), and in these the index α was determined. Fig. 4 illustrates the principal optical and morphological features of clinoenstatite as described in the literature, and confirmed in the course of this investigation. The curve used for the determination of composition was that published by Hess (1949, p.643); it is more or less the same as that of Bowen and Schairer (1953, p.198), which differs in expressing composition in weight percent. Bowen and Schairer's curves in fact give values of $FeSiO_3$ about 2 molecular percent lower. The results of the measurements are set out in Table 3; all values are subject to an error of $\pm$ 0.001.

Table 3 →

Taking into account a possible error of 0.001 at either extreme of the values given, the possible range of composition in specimen LB107 would be 9 to 12 molecular percent $FeSiO_3$, and in LB105, 8.5 to 10 percent. Most grains showed a slight variation of refractive index along their lengths, i.e., parallel to c. Interference colours are first order yellow.

No systematic refractive index measurements were made on bronzite; the only value obtained was a mean reading for use in correcting optic axial angles. This was about the same in both rocks - 1.670, or a little more.

TABLE 3

Refractive index measurements on clinoenstatite phenocrysts.

	α	Composition (mol. % $FeSiO_3$)
LB107	1.662[1]	9.5
	1.663	10.5
	1.664[1]	11
LB105	1.661(5)[2]	9

1. Two identical measurements
2. Three identical measurements

Measurements of 2V in clinoenstatite were carried out on sections cut more or less at right angles to c (Fig. 4), and wherever possible the angle was measured in both sets of lamellae; where this could be done, a value for $\gamma \wedge c$ was obtained by the method of Turner (1942) - $\gamma \wedge c = \frac{\gamma_1 \hat{\ast} \gamma_2}{2}$. Measurement was often difficult or entirely unsuccessful, and there were three reasons for this - the very small difference between α and β (especially in crystals with 2V = 30° ±), the narrowness of the twin lamellae, and interference from lamellae on either side of the one under examination.

Fig. 4 =>

The most reliable readings for $\gamma \wedge c$ ranged from 28° to 31°

The clinoenstatite is optically positive. Two sets of values for 2V were obtained - one of 25° - 36° (± 2° for measurements on individual grains), and the other of 46° - 56° (± < 0.5° for measurements on individual grains). One quite satisfactory determination, carried out on the crystal illustrated in Plate 1, fig. B, gave an intermediate reading of 41°. The values for 2V are different from those (20° - 25°) given by Bowen and Schairer (1935, p. 198) for the clinoenstatite-clinoferrosolite series. However, one set (46° - 56°), straddles the value of 53.5° given by Allen and White (1909) and Atlas (1952) for pure clinoenstatite, and also virtually covers the values 44° ± 2 ° and 50° ± 5° given by Turner, Heard, and Griggs (1960) for clinoenstatite formed by stress-induced inversion from enstatite in enstatite pyroxenite. The lower values were obtained from some of the larger phenocrysts, whereas most of the higher values were obtained on the small crystals

described on page 16, and illustrated in Plate 2, fig. A., Plate 3, fig. C, and Fig.3. Results of some of the measurements of 2V and extinction angles are set out in Table 4. In general the absence of readings for $\gamma \wedge c$ signifies that measurements were not made on the second set of twin lamellae.

Table 4 ->

Symmetrical extinction of 29.5° was measured on the crystal shown on the left side of Fig. C, Plate 1. According to the curve shown by Hess (1952, p. 643) this value corresponds to a composition of 10.5 molecular percent of $FeSiO_3$, which is the same as the mean composition obtained by R.I. measurements on phenocrysts from the same specimen (Table 3).

As mentioned previously, bronzite phenocrysts are commonly zoned, and so the simplest method of getting some idea of their composition was by measurement of 2V. The results of the determinations are shown in Table 5; the curves used are those given by Hess (1952).

Table 5 ->

From Table 5 it can be seen that:

(a) If the compositions of unzoned phenocrysts and small crystals obtained by direct measurement of 2V in specimen LB107 are averaged, they are found to be the same (11 molecular percent $FeSiO_3$) as those of the single phenocryst and the single small crystal reliably measured in LB105.

(b) In most simply zoned phenocrysts (e.g., Nos 5, 6, 8) the core is more iron-rich than the outer zone (cf. electron microprobe results for bronzite - Table 8).

TABLE 4

Optic axial angles and extinction angles in clinoenstatite.

	$2V_y$	$y \wedge c$
LB107	31°	-
	30°	-
	34°	-
	32°	26° ?
	36°	31°
	41°	29°
	53°	-
	56°	-
	49°	24° ?
	47°	23° + ?
	46°	28°
	51°	28°
LB105	25°	-
	31°	-
	27°	29°
	55°	Not measurable

TABLE 5

Optic axial angles and composition of orthopyroxene.

		(a) Phenocrysts		Composition (Mol. % $FeSiO_3$)	
		Measured	Plotted	From measured	From plotted
		2Vα	2Vα	2Vα	2Vα
LB107	(1) Core	-	83°	-	16 ?
	Zone 1	-	73°	-	22 ?
	Zone 2	-	87°	-	14 ?
	Zone 3	-	77°	-	20 ?
	(2)	95° ?	99°	10-	8.5 ?
	(3)	92°	99°	12	8.5)
			85°		15) 12
	(4)	91°+	93°	12-	11 ?
LB105	(5) Core	79°	-	18	-
	Outer zone	96°	-	10	-
	(6) Core	92°	-	12	-
	Outer zone	97°	-	9	-
	(7)	93°	-	11	-
	(8) Core	87°	-	14	-
	Outer zone	94°	-	10.5	-
		(b) Small Crystals (Plate 2, fig.A; Plate 3, fig.C; Fig. 3)			
LB107	(9)	91°	-	12	-
	(10)	95°	90°	10	13)
			101°		8) 10.5
	(11)	99°	-	8.5	-
	(12)	89°	97°	13	9)
			81°		17) 13
LB105	(13) Core	-	99°	-	8.5 ?
	Outer zone	-	85°	-	15 ?
	(14)	94°+	91°	11-	12 ?

(c) The only measured example (No.13) of a small zoned crystal is in LB105; this grain differs from the zoned phenocrysts in that its outer zone is more iron-rich than the core.

X-RAY DIFFRACTION DATA. (D.H.G.)

In Table 6, the d-spacings for the major reflections of a clinoenstatite phenocryst are listed and compared with equivalent reflections from synthetic clinoenstatite (Kuno and Hess, 1953) and synthetic clinoferrosilite (Lindsley, Davis, and MacGregor, 1964). The correspondence between the patterns is clear, and the differences between the natural clinoenstatite and the synthetic clinoenstatite appear consistent with the effect of the $FeSiO_3$ substitution in the former.

Table 6

ELECTRON PROBE MICRO-ANALYSIS. (D.H.G.)

Method:- An electron probe X-ray micro-analyser (Applied Research Laboratories model E.M.X.) was used to quantitatively analyse for selected elements in a number of the clinoenstatite and orthopyroxene (bronzite) phenocrysts. Polished thin sections of rocks LB105 and LB107 were prepared, and coated with a thin carbon film. The electron beam was focussed to a spot about 1 micron in diameter, giving a volume of analysis (the volume from which characteristic X-rays

TABLE 6

X-ray data for a Cape Vogel clinoenstatite phenocryst. Ni - filtered Cu $K\alpha$ radiation, Si internal standard, Phillips diffractometer.

	Synthetic Clinoenstatite (Kuno and Hess, 1953)		Natural Clinoenstatite (This work)		Synthetic Clinoferrosilite (Lindsley, Davis, MacGregor, 1964)	
hkl	'd' - spacing	I	'd' - spacing	I	'd' - spacing	I
021	3.287	5	3.293	1	3.345	8
220	3.174	6	3.178	8	3.233	8
$22\bar{1}$	2.980	9	2.986	6	3.033	10
310	2.878	10	2.880	10	2.910	6
$13\bar{1}$	2.542	3	2.547	3	2.604	3
$20\bar{2}$	2.524	3	2.526	1	2.595	2
002	2.459	6	2.459	4	2.481	2
	-		2.453	1		
221	2.436	2	2.439	3	2.476	2
	2.379	2	2.380	1		
			2.280	½		
311	2.213	2	2.210	5		
040	2.208					
					2.161	2
					2.038	2

were emitted) of 2-3 microns diameter. The accelerating voltage on the electron beam was 12 kV, and the specimen current 0.04 micro-amps. Spot analyses were made at intervals of 1 micron to 10 microns with an integration time of 70 seconds. Analyses for Fe, Ca, and either Al or Mg were made simultaneously using Kα radiation. Corrections were made for beam current fluctuations and for background, but inter-element and matrix absorption and fluorescence effects were minimised by using calibration curves from glasses of known pyroxene composition. These standard glasses, prepared from carefully weighed oxide mixes, are enstatite (En_{90}) with 2.0% CaO and variable Al_2O_3 content from 0 - 20%, and aluminous hypersthene (En_{75}, Al_2O_3 = 8.0%) with variable CaO content from 0 - 8%. The determinations of Fe, Ca, and Al (reported in Tables 7, 8, and 9 as the oxides in accordance with normal petrographic practice) are considered accurate to $\pm$ 0.1%, this estimate being derived from the reproducibility of results on both standards and sample, and the linearity of the calibration curve. Determinations of Mg showed greater effects of small machine fluctuations, and the estimated error is $\pm$ 0.3%. Where Fe, Ca, Mg, and Al were measured on the same crystal it is possible to calculate the remainder of the composition assuming that these three elements occur in the pyroxene as $FeSiO_3$, $CaSiO_3$, $MgSiO_3$, and Al. AlO_3. Totals calculated in this way range from 99.3 to 100.0, in excellent agreement with the ideal compositions. $MnSiO_3$, $NiSiO_3$, and Cr_2O_3 are likely to total to less than 0.5% in pyroxenes of this composition.

Results:- Series of 4 to 10 spot analyses at 5 or 10 micron intervals were made near the centres of several clinoenstatite and orthopyroxene phenocrysts in each of the two rocks. These demonstrate that there is a range in composition of clinoenstatite and orthopyroxene in both rocks, but that the orthopyroxene is consistently more iron-rich and calcium-rich than the clinoenstatite (Tables 7, 8, and 9; Fig. 5).

A further series of very detailed traverses from margin to centre or opposite margin of selected phenocrysts of both types demonstrates extremely strong compositional zoning at the outermost edges of the phenocrysts, but only very slight or moderate zoning within the phenocrysts. Orthopyroxene of the type illustrated in Plate 2, fig. B shows moderate zoning (Table 8, Nos. 10 and 12), or slight zoning (Table 8, Nos. 1 and 5). Some clinoenstatite has very little zoning (Table 7, No. 16), but in both pyroxenes the outer zones of the crystal are more magnesian than the central core. This same trend is shown by the composite crystals (Plate 2, figs. C and D) consisting of a hypersthene core and an outgrowth of or partial mantle of clinoenstatite. Analyses of the crystals illustrated in Plate 2, figs. C and D are given in Table 9, Nos. 1 and 4, and Table 8, bronzites Nos. 3 and 5. Some of these crystals have a small included grain of clinoenstatite at their centres (e.g., Plate 2, figs. D and E; Fig. 6; Table 9, Nos. 3 and 4).

TABLE 7

Microprobe analyses of clinoenstatite

		Weight per cent						Mol. per cent		
	LB105	FeO	CaO	MgO	Al_2O_3	$FeSiO_3$	$CaSiO_3$	$MgSiO_3$	Fe	Ca	Mg
1	Clinoenstatite core	7.1	0.2	34.3	0.5	13.1	0.4	85.4	10.3	0.4	89.3
2	"	7.7	0.2	n.d.	0.4	14.1	0.4	85.1	11.2	0.4	88.4
3	"	6.7	0.15	n.d.	0.3	12.3	0.3	87.1	9.7	0.3	90.0
4	"	6.0	0.15	n.d.	0.4	11.0	0.3	88.3	8.7	0.3	91.0
5	"	7.4	0.2	n.d.	0.4	13.6	0.4	85.6	10.7	0.4	89.0
6	"	7.9	0.2	n.d.	0.4	14.5	0.4	84.7	11.5	0.4	88.1
7	"	5.6	0.15	n.d.	0.6	10.3	0.3	88.8	8.1	0.3	91.6
8	"	7.9	0.2	n.d.	0.6	14.5	0.4	84.5	11.5	0.4	88.1
9	"	7.0	0.3	n.d.	0.5	12.9	0.6	86.0	10.1	0.5	89.4
	LB107										
10	Clinoenstatite core	7.7	0.2	34.2	0.4	14.1	0.4	85.1	11.1	0.4	88.5
11	"	8.6	0.2	33.7	n.d.	15.8	0.4	83.9	12.6	0.4	87.0
12	"	8.2	0.1	n.d.	n.d.*	15.1	0.2	84.2	11.9	0.2	87.9
13	"	8.2	0.2	n.d.	0.4	15.1	0.4	84.1	11.9	0.4	87.7
14	"	8.1	0.2	n.d.	0.4	14.9	0.4	84.3	11.8	0.4	87.8
15	"	8.1	0.2	n.d.	0.4	14.9	0.4	84.3	11.8	0.4	87.8
16	Large clinoenstatite averaged over 50 μ intervals,										
a	Margin	7.7	0.15	n.d.	0.5	14.2	0.3	85.0	11.2	0.3	88.5
b		7.7	0.15	n.d.	0.6	14.2	0.3	84.9	11.2	0.3	88.5
c		7.9	0.15	n.d.	0.6	14.5	0.3	84.6	11.5	0.3	88.2
d		8.1	0.2	n.d.	0.7	14.9	0.4	84.0	11.8	0.4	87.8
e		8.2	0.2	n.d.	0.5	15.1	0.4	84.0	11.9	0.4	87.7
f		8.0	0.25	n.d.	0.5	14.7	0.5	84.3	11.6	0.4	88.0
g	Centre	8.1	0.15	n.d.	0.4	14.9	0.3	84.4	11.8	0.3	87.9

* assumed 0.5%

TABLE 8

Microprobe analyses of orthopyroxene

	Weight per cent							Mol. per cent		
	FeO	CaO	MgO	Al_2O_3	$FeSiO_3$	$CaSiO_3$	$MgSiO_3$	Fe	Ca	Mg
LB105										
1. Bronzite(zoned)										
a Outer Margin	10.2	0.9	31.5	0.9	18.7	1.9	78.3	15.1	1.7	83.2
b	10.4	0.9	31.3	0.9	19.1	1.9	77.9	15.4	1.7	82.9
c Core Centre	10.6	0.95	31.1	0.9	19.5	2.0	77.3	15.8	1.8	82.4
2. Bronzite	8.9	0.7	n.d.	0.6	16.3	1.5	81.6	13.1	1.3	85.6
3 "	8.9	0.65	n.d.	0.6	16.3	1.4	81.7	13.1	1.3	85.6
4 "	10.0	0.8	n.d.	0.9	19.5	1.9	77.8	15.8	1.7	82.5
5 Bronzite (zoned)										
a Margin	9.7	1.0	n.d.	0.7	17.8	2.1	79.4	14.3	1.9	83.8
b	9.0	0.9	n.d.	0.8	16.5	1.9	80.8	13.2	1.7	85.1
c	8.9	0.9	n.d.	0.8	16.3	1.9	81.0	13.1	1.7	85.2
d	8.9	0.9	n.d.	0.7	16.3	1.9	81.1	13.1	1.7	85.2
e	8.8	0.9	n.d.	0.75	16.2	1.9	81.3	13.0	1.7	85.3
f	8.9	0.85	n.d.	0.7	16.3	1.8	81.2	13.1	1.6	85.3
g	8.8	0.9	n.d.	1.0	16.2	1.9	80.9	13.0	1.7	85.3
h	9.2	1.0	n.d.	1.0	16.9	2.1	80.0	13.6	1.9	84.5
i Opposite margin	9.4	1.0	n.d.	1.3	17.2	2.1	79.4	14.0	1.9	84.1
LB107										
6 Bronzite	9.4	0.7	n.d.	0.7	17.2	1.5	80.6	13.8	1.3	84.9
7 "	9.8	0.7	n.d.	0.5	18.0	1.5	80.0	14.4	1.3	84.3
8 "	9.1	0.6	n.d.	0.5	16.7	1.2	81.6	13.3	1.2	85.5
9 "	9.9	0.85	n.d.	1.1	18.2	1.8	78.9	14.7	1.6	83.7
10 Bronzite (strongly zoned)										
a Outer Margin	9.4	0.7	n.d.	0.7	17.2	1.5	80.6	13.8	1.3	84.9
b	10.5	0.8	n.d.	0.7	19.3	1.7	78.3	15.5	1.5	83.0
c Centre	11.4	1.1	n.d.	1.1	20.9	2.3	75.7	17.1	2.1	80.8
11 Bronzite	9.7	0.6	32.8	n.d.	17.8	1.2	81.7	14.2	1.2	84.6
12 Bronzite (zoned)										
a Margin	9.7	0.7	32.5	n.d.	17.8	1.4	81.4	14.2	1.3	84.5
b	11.2	0.9	31.1	n.d.	20.6	1.9	77.4	16.6	1.7	80.7
c	14.5	1.4	28.6	n.d.	26.6	2.9	71.2	21.8	2.7	75.5
d Opposite Outer zone margin	9.5	0.7	32.5	n.d.	17.5	1.4	80.9	13.9	1.3	84.8
13 Bronzite	8.8	0.65	n.d.	n.d.*	16.2	1.3	82.0	12.9	1.2	85.9
14 "	9.2	0.9	n.d.	n.d.*	16.9	1.9	80.7	13.5	1.7	84.8
15 "	9.3	0.9	n.d.	n.d.*	17.1	1.9	80.5	13.6	1.7	84.7
16 "	9.5	0.9	n.d.	n.d.*	17.4	1.9	80.2	13.9	1.7	84.4

* assumed 0.5%.

TABLE 9

Microprobe analyses of composite pyroxene crystals.

	Weight per cent.							Mol. per cent.			
	FeO	CaO	MgO	Al_2O_3	$FeSiO_3$	$CaSiO_3$	$MgSiO_3$	Fe	Ca	Mg	Associated grain.
LB105											
1. Clinoenstatite rim	6.9	0.3	n.d.	0.8	12.7	0.6	85.9	10.0	0.5	89.5	Bronzite No. 3, Table 8
2. ½Clinoenstatite	6.7	0.2	n.d.	0.5	12.3	0.4	86.8	9.7	0.4	89.9	Bronzite No.2, Table 8
Opposite edge of Bronzite	7.3	0.55	n.d.	0.6	13.4	1.1	84.9	10.6	1.0	88.4	
3. (?)Clinoenstatite rim	7.5	0.4	33.8	0.5	13.8	0.8	84.2	11.2	0.7	88.1	Bronzite No.1, Table 8
Included clinoenstatite	8.1	0.1	33.7	0.6	14.9	0.2	83.9	11.8	0.2	88.0	
(?)Clinoenstatite rim	8.25	0.1	n.d.	0.6	15.1	0.2	84.1	12.1	0.2	87.7	
4. Clinoenstatite rim	6.8	0.2	n.d.	0.4	12.5	0.4	86.7	9.9	0.4	89.7	Bronzite No.5, Table 8
Included Clinoenstatite	8.1	0.3	n.d.	1.0	14.9	0.6	83.5	11.9	0.5	87.6	
Opposite rim (inner)	7.1	0.3	n.d.	0.4	13.0	0.6	86.0	10.3	0.5	89.2	
(outer)	6.4	0.2	n.d.	0.4	11.7	0.4	87.5	9.2	0.4	90.4	
LB107											
5. ½Clinoenstatite											
a - Centre	8.15	0.2	n.d.	0.9	15.0	0.4	83.7	11.9	0.4	87.7	
b - Near Bronzite	8.85	0.2	n.d.	0.65	16.25	0.4	82.7	12.9	0.4	86.7	
½ Bronzite	9.4	0.7	n.d.	0.7	17.2	1.5	80.6	13.8	1.3	84.9	
6. Part Clinoenstatite	8.7	0.35	n.d.	0.8	16.0	0.7	82.5	12.9	0.6	86.5	
	8.7	0.3	n.d.	0.6	16.0	0.6	82.8	12.8	0.5	86.7	
Part Bronzite	9.4	0.7	n.d.	0.7	17.3	1.4	80.6	13.8	1.3	84.9	
	9.3	0.7	n.d.	0.6	17.1	1.4	80.9	13.6	1.3	85.1	
7. Untwinned central part of very elongate small crystal	7.6	0.55	n.d.	0.6	14.0	1.1	85.3	11.0	1.0	88.0	
8. Microlite	18.0	4.45	22.8	n.d.	33.0	9.2	56.8	28.0	8.8	63.2	
9. Microlite	18.0	5.8	22.0	n.d.	33.0	12.0	54.8	27.9	11.4	60.7	

The zoning at the outermost edge of the crystals is towards more iron-rich pyroxene with slightly increased lime content, and then there is an abrupt change to a rim of augitic composition (Figs. 6, 7, 8). In some cases this outermost calcic clinopyroxene zone has a sharp boundary with the inner Ca-poor pyroxene, and the analytical points in Figs. 6, 7, and 8, which occur within the normal pyroxene miscibility gap, reflect the finite size of the analyzed spot crossing a sharp 2-phase boundary, and do not represent true compositions of a single-phase pyroxene.

Figs 6, 7, 8 with Nos. 8 & 9.

A number of traverses were made across small composite phenocrysts of orthopyroxene and clinoenstatite. Such crystals are shown in the upper half of Plate 2, fig. C, in Plate 3, fig. C., and diagrammatically in Fig. 4. Results of analyses are given in table 9, Nos. 2, 5, and 6. Again there is a consistent difference between the two pyroxene types, but it is clear from tables 7, 8, and 9 that these composite grains consist of pyroxenes near the limiting Fe-end of the clinoenstatite field and the limiting Mg-end of the orthopyroxene field. Thus, although the types are distinct structurally they converge towards a common limit to their respective composition fields.

Attempts were made to measure several of the microlites, but with little success - two examples (Table 9, Nos. 8 and 9) gave molecular ratios Mg : Fe : Ca of 63.2 : 28.0 : 8.8 and 60.7 : 27.9 : 11.4, and thus fall in the pigeonite field.

Almost all the orthopyroxene phenocrysts showed a distinct

narrow zone rich in Mg at their margins. In the crystals illustrated in Plate 2, figs. C and D, this zone is of the same chemistry as the clinoenstatite phenocrysts, and shows polysynthetic twinning. In some crystals there is a very thin zone with Mg and Fe contents typical of clinoenstatite, but with higher Ca content (CaO = 0.4% to 0.55%, Table 9, Nos. 2 and 3; see also Fig. 6). These zones do not show polysynthetic twinning. A small, very thin, elongate crystal (similar to that shown in Plate 3, fig. B) with an outer zone of twinned clinoenstatite contains a clear, untwinned core with CaO = 0.55% (Table 9, No. 7), but Mg and Fe contents typical of the clinoenstatites. These three examples (see also Fig. 5) are exceptions to a generalization that phenocrysts with $\frac{Mg}{Mg + Fe}$ molecular ratios greater than 87 show polysynthetic twinning, clinoenstatite structure, and very low lime content (0.1% to 0.3% CaO).

A Ca-Mg-Fe plot (molecular proportions) of the analyzed pyroxenes is given in Fig. 5. The clinoenstatite phenocrysts range from at least 92% to 87% Ens, and contain 0.2% to 0.5% Wo. They are very low in Al_2O_3 (averaging about 0.5 weight per cent) in spite of their high temperature of formation; this presumably reflects the low Al_2O_3 content of the whole rock and a low confining pressure at crystallization. The low Al_2O_3 content suggests that the phenocrysts are not inherited from great depth (i.e., below 20-30 km).

Phenocrysts more iron-rich than $\frac{Mg}{Mg + Fe} = 87$ have normal

orthopyroxene structure, and range from En_{87} to En_{78}, with Wo-content increasing from 1.2% to 2.7% (0.6% to 1.4% CaO) in the more iron-rich examples. Al_2O_3 content is again low (averaging about 0.9%), but is higher than that of the clinoenstatites.

Interpretation:- In the simple system $MgSiO_3$ - $FeSiO_3$ Bowen and Schairer (1935) have shown that there is a complete solid solution series at high temperature between clinoenstatite and clinohypersthene of composition near En_{10} Fs_{90}. On the other hand, later experimental work (Atlas, 1952) has shown that clinoenstatite is a metastable phase in a low-pressure, high-temperature environment, and forms by inversion from the high-temperature polymorph, protoenstatite. The stable inversion is from protoenstatite to orthoenstatite, and experimental studies show that this occurs in pure $MgSiO_3$ at 985°C ± 10° (Atlas, 1952; Boyd and Schairer, 1964). Clinoenstatite has a stability field at very low temperatures and high pressures (Solar, Carrison, and Schwartz, 1964). Although 985°C ± 10°C is the temperature for the inversion protoenstatite $\rightleftharpoons$ orthoenstatite in pure $MgSiO_3$ composition, the effect of Fe solid solution in the pyroxene is unknown. Boyd and Schairer (1964, p. 308) present alternative phase diagrams for $MgSiO_3$ - $FeSiO_3$ compositions in which the temperature of inversion either increases or decreases with increasing $FeSiO_3$ content.

It may be pointed out that a phase diagram in which the temperature of the protoenstatite-orthoenstatite inversion decreases

with increasing $FeSiO_3$ content (the first alternative, Fig. 11B, of Boyd and Schairer, 1964) is not supported by the data here presented. We may assume that the liquidus temperature of the rock decreases with increasing Fe content, and that of the two phenocryst types orthopyroxene crystallized at the lower temperature. If the inversion temperature decreased with increasing $FeSiO_3$ substitution, then the temperature at which orthopyroxene crystallized would be appreciably less than 985°C. The data of Tilley, Yoder, and Schairer (1964), discussed below, demonstrate that whereas protoenstatite is in equilibrium with liquid at 1250°C in the whole rock, orthoenstatite is in equilibrium with liquid at 1150°C, so that the inversion temperature for a pyroxene probably around En_{85-90} lies between 1150°C and 1250°C.

Tilley, Yoder, and Schairer (1964) have reported some preliminary results of experimental melting on the rock LB107. They found that, in the dry rock, protoenstatite was the liquidus phase at 1385°C, and that protoenstatite was still the only phase crystallizing in a 14 day run at 1250°C. The difference in composition between the protoenstatites at the two temperatures is unknown. Shorter runs at 1250°C produced orthoenstatite with clinoenstatite, the former apparently being a metastable inversion from clinoenstatite (Tilley, Yoder, and Schairer, 1964). When held for 7 days at 1150°C there were abundant euhedral orthoenstatite phenocrysts accompanied by minor calcic clinopyroxene set in glass.

The experimental work supports the conclusion that the

magnesium metasilicate phase originally crystallized from the liquid as protoenstatite, but inverted to clinoenstatite at a lower temperature (perhaps about 860°C (Sarver and Hummel, 1962)). The temperature at which protoenstatite crystallized cannot be specified, as the magma apparently had a high volatile content, and liquidus temperatures may have been lower than those found by Tilley, Yoder, and Schairer.

The composition of the Cape Vogel clinoenstatite may reflect exactly the composition of the primary protoenstatite. If this is so then the protoenstatite is distinctive in its extremely low CaO content. This is in harmony with the findings of Boyd and Schairer (1964, pp. 290-296) that protoenstatite crystallized in equilibrium with calcic clinopyroxene at temperatures near the protoenstatite $\rightleftharpoons$ orthoenstatite inversion curve contains much less CaO than orthoenstatite immediately below the inversion curve.

Alternatively, CaO may have exsolved from the protoenstatite during inversion. Such an interpretation would suggest a continuity of compositions of phenocrysts in the Ca - Mg - Fe diagram (Fig.5). Some evidence in support of this is found in the few crystal margins and one microlite core composition which plot with the clinoenstatites in $\frac{Mg}{Mg + Fe}$ content, but are higher in Wo content, and lie close to the extrapolation from the orthopyroxene trend. However, there is no evidence in the microprobe data for exsolution from the clinoenstatite; detailed traverses, even at 1 - 2 micron intervals,

did not reveal lamellae of Ca-rich clinopyroxene.

The presence of two phenocryst types (clinoenstatite inverted from protoenstatite and the orthopyroxene), with consistent compositional differences between them, leads to the conclusion that, during growth of the phenocrysts, the magma temperature moved through the protoenstatite $\rightleftharpoons$ orthoenstatite inversion curve. The liquidus curve of the magma intersected the pyroxene inversion curve at the point where the pyroxene crystallizing had a molecular ratio $\frac{Mg}{Mg + Fe} = 87$. Fig. 9 shows a liquidus curve consistent with the observed features of the rock, and a relationship between pyroxene polymorphs in the natural $MgSiO_3 - FeSiO_3$ system similar to that suggested by Boyd and Schairer (1964, p. 308, Fig. 11A).

Fig. 9 →

From the analytical data on the pyroxenes, it is clear that the magma crystallized in two distinct stages. The first stage gave rise to free growth of phenocrysts, and the reverse zoning of these is possibly due to a temperature rise during crystallization, perhaps in the uppermost parts of the magma conduit. This stage was followed by one of very rapid crystallization with formation of many pyroxene nucleii and microlites, and by sharp normal zoning on the margins of phenocrysts. During this stage the Ca-poor pyroxene probably moved into the pigeonite field, and was joined by a Ca-rich augite, commonly nucleating on the phenocryst margins, and containing 35 - 40 mol. % wollastonite. Finally the remaining liquid chilled to a glass + a volatile-rich phase.

PETROGENESIS. (W.B.D., J.E.T.)

In seeking reasons why clinoenstatite has not previously been found in volcanic rocks, consideration must be given to the more unusual compositional features of the specimens here described. Of prime importance in this connection are the high magnesia percentage relative to that of silica, the high Mg/Fe^{++} ratio, and probably also the high water content (possibly up to 7 percent, assuming that it is valid to include most of the water lost at 110°C *). The abundant water could be expected to lower the liquidus temperature, thus allowing protoenstatite to crystallize at temperatures appreciably lower than those recorded for dry melts.

The high Mg/Fe^{++} ratio caused protoenstatite to crystallize in preference to pigeonite (see Fig. 9), and the high Mg/Ca ratio

---

* It is interesting to note that the ratio -

$$\frac{H_2O - (LB107)}{H_2O - (LB105)} = \frac{1}{1.56}$$

is approximately equal to the ratio -

$$\frac{\text{Zeolites + altered glass (LB107)}}{\text{Zeolites + altered glass (LB105)}} = \frac{1}{1.65} ;$$

two interpretations of this feature seem possible - either the zeolites and altered glass lost some of their combined or contained water at 110°C, or they absorbed water when powdered. LB105 contains a higher proportion of strongly altered glass than does LB107.

prevented crystallization of Ca-rich clinopyroxene as phenocrysts. The unusually low Al/Ca ratio, relative to silica percentage, effectively inhibited the crystallization of plagioclase. Some of the lime entered late clinopyroxenes, and because of the high water content of the residual magma much of the remaining lime and alumina, together with soda, crystallized as zeolites in the final stages of cooling.

The presence of this unique rock in a tectonically mobile zone between relatively stable continental and oceanic crustal elements invites speculation as to whether it was generated directly in the upper mantle, or formed by assimilation of magnesium-rich ultramafic rock by acid magma, or by assimilation of acid igneous rock by substantially liquid, magnesium-rich ultramafic magma (whose existence in now generally considered to be unacceptable (Turner and Verhoogen, 1960, pp. 313-316)), or by mixing of magnesium-rich ultramafic magma and acid magma. The considerable compositional variability noted in the clinoenstatite-bearing rock (see Addendum, p. 305) appears to favour assimilation or mixing rather than generation in the upper mantle without substantial contamination, especially as the rock composition lies well away from the normal lines of magmatic differentiation.

It is obvious that the final (hybrid) magma must have been completely liquid, except for xenoliths, and that it must have reached a temperature above 1150°C (Tilley, Yoder, and Schairer, 1964) for protoenstatite to have crystallized. Whether this magma formed by

assimilation of solid rock or by mixing of different magmas, it seems necessary to assume (at least) one of two special conditions - conditions contradictory to currently held concepts of petrogenesis based on field, and petrographic, and experimental studies. These conditions are :

(1) Strong superheating within acid or intermediate magma to allow assimilation of ultramafic rock on an appreciable scale.

(2) The existence of a substantially liquid ultramafic magma to permit assimilation of acid or intermediate rock, or mixing with acid or intermediate magma.

The optimum situation for generation of the hybrid magma would result from coexistence of both these conditions, and it is possible that exceptional geological situations could have developed in north-eastern Papua in early Tertiary time, when tectonic activity associated with the emplacement of the Papuan Ultrabasic Belt (Thompson, 1957; Dow and Davies, 1964) was intense.

Trial calculations suggest that the types of rocks or magmas which could give rise to an end-product of the desired composition must be fairly restricted, viz.:

(1) More or less equal quantities of quartz diorite and bronzitite or hypersthenite (preferably wholly or partly serpentinized - see below). The quartz diorite would have to be a lime-rich and rather unusually iron-rich variety unless the orthopyroxenite

were fairly rich in iron, and contained some diopside.

(2) More or less equal quantities of granodiorite and diopside- and hypersthene-bearing peridotite (or serpentinite derived therefrom. Assimilation of serpentinite could account for the high water content of at least some of the clinoenstatite-bearing rock, and digestion of serpentinized rock would take place at appreciably lower temperatures than those required for anhydrous peridotite or bronzitite).

Specimen LB107 contains several small aggregates of bronzite grains (p.14) which could be remnants of modified ultramafic inclusions. The appearance of individual grains in the aggregates is quite different from that of the bronzite phenocrysts, and some of them contain probably ex-solution lamellae of clinopyroxene, a feature not found in the phenocrysts or the microlites. This suggests that the aggregates may not have crystallized directly from the melt which was the immediate source of the phenocrysts. In this connection it is interesting to find that Baker (1946, p.25) suggested that the notably high (8%) magnesia content of andesite from Waiowa volcano may be due to contamination of "a moderately acid magma" by "xenocrysts of magnesia-rich minerals derived from... ultrabasic basement rock..."

Suggestions here put forward for the genesis of the

clinoenstatite-bearing rocks at Cape Vogel originated in trial calculations based on possible or actual chemical compositions of igneous rock-types that are known or could reasonably be expected to exist - either at the surface or at depth - in the area between Mount Lamington and Milne Bay. We are aware that important theoretical and practical difficulties arising from current ideas on petrogenesis must be met, and that our suggestions can only be regarded as speculative at this stage. However, the question of genesis will be kept in mind as investigation of the clinoenstatite-bearing rocks continues, and we hope that a study of inclusions within them and other igneous rocks in the vicinity, as well as information from additional chemical analyses, will provide useful guides to a satisfactory solution.

ACKNOWLEDGMENTS

We are grateful to Professor C.E. Tilley for encouraging us to prepare this paper, and for critically reading the manuscript.

The two authors from the Bureau of Mineral Resources wish to thank its Director, Mr. J.H. Rayner, for permission to publish their contributions. They are indebted to Dr. A.J.R. White, of the Australian National University, and W.R. Morgan, of the Bureau of Mineral Resources, for checking some of the optical measurements, to S.C. Goadby for X-Ray powder identification of the aragonite, and to G. Millist, E.J. Zawartko, F.J. Roberts, and P.R. Brown for help in the preparation of illustrations.

Thompson and Dallwitz also wish to express their gratitude to members of the Anglican Mission at Tarakururu for help and hospitality during a visit to Cape Vogel in 1964.

ADDENDUM. (G.B.D.)

In June and July, 1964, Thompson and Dallwitz revisited the clinoenstatite locality to collect more specimens, and to carry out additional mapping in the immediate vicinity. During this visit crystals of clinoenstatite up to 2.5 cm. long and about 4 mm. wide were noted. Preliminary examination of thin sections shows that the composition of the rock-mass is variable. Some of the variations are listed below:

Orthopyroxene phenocrysts about three times as plentiful as those of clinoenstatite.

Clinoenstatite phenocrysts 60% to 65% of rock; very little orthopyroxene.

Clinoenstatite phenocrysts and microlites together make up at least 75% of rock; no orthopyroxene and no zeolites.

Clinoenstatite 70% of rock; no orthopyroxene or zeolites; talc pseudomorphs after probable olivine.

Cores of clinoenstatite phenocrysts altered to talc.

Zeolites absent in unaltered varieties with small phenocrysts; some opal present.

Zeolites locally more abundant than in LB105 and LB107, and commonly accompanied by chalcedony and/or quartz (up to

10% of rock) as vesicle fillings; rocks containing zeolites and silica are more altered than those containing zeolites only, and veins of quartz and brown chalcedony are locally abundant where they outcrop. Clinoenstatite may be completely altered, orthopyroxene fresh.

REFERENCES

Allen, E.T., White, W.P., Wright, F.E. and Larsen, E.S., 1909. Diopside and its relation to calcium and magnesium metasilicate. Amer. J. Sci. 4th Ser. 27, 1-47.

Atlas, L., 1952. The polymorphism of $MgSiO_3$ and solid state equilibria in the system $MgSiO_3$ - $CaMgSi_2O_6$. J. Geol. 60, 125-47.

Anglo-Persian Oil Company, 1930. The oil exploration work in Papua and New Guinea, 1920-1929. Rept. to the Commonwealth Government of Australia, Vol II. (unpublished).

Baker, G., 1946. Preliminary note on volcanic eruptions in the Goropu Mountains, southeastern Papua, during the period December, 1943, to August, 1944. J. Geol. 54, 19-31.

Belford, D.J., 1959. Lower Miocene foraminifera from the Milne Bay area, Papua. Bur. Min. Resour. Aust. Rec. 1959/99 (unpublished).

Binns, R.A., Long, J.V.P., and Reed, S.J.B., 1963. Some naturally occurring members of the clinoenstatite-clinoferrosilite mineral series. Nature 198, 777-8.

Bowen, N.L., and Schairer, J.F., 1935. The system MgO-FeO-SiO_2. Amer. J. Sci. 29, 151-217.

Boyd, F.R., and Schairer, J.F., 1964, The system $MgSiO_3$ - $CaMgSi_2O_6$. J. Petrol. 5, 275-309.

Crespin, I., and Belford, D.J., 1955. Micropalaeontological examination of rock samples from the Cape Vogel area, Papua. Bur. Min. Resour. Aust. Rec. 1955/56 (unpublished).

Crespin, I., Kleinski, F.M., Paterson, S.J., and Belford, D.J., 1956. Papers on Tertiary micropalaeontology. Bur. Min. Resour. Aust. Rep. 25.

Davies, H.L., and Ives, D.J., 1965. The geology of Fergusson and Goodenough Islands, Papua. Bur. Min. Resour. Aust. Rep. 82.

De Roever, W.P., 1957. Sind die alpinotypen Peridotitmassen vielleicht tektonisch verfrachtete Bruchstücke der Peridotitschale? Geol. Rundschau 46, 137-146.

Dow, D.B., and Davies, H.L., 1961. The geology of the Bon. Mountains, New Guinea. Bur. Min. Resour. Aust. Rec. 1961/84 (unpublished); subsequently published 1964, Rep. 75.

Foster, W.R., 1951. High temperature X-ray diffraction study of the polymorphism of $MgSiO_3$. J. Amer. Ceram. Soc. 34, 255-9.

Glaessner, M.F., 1950. Geotectonic position of New Guinea. Bull. Amer. Assoc. Petrol. Geol. 34, 856-881.

Green, D.H., 1961. Ultramafic breccias from the Musa Valley, Papua. Geol. Mag. 98, 1-26.

Hess, H.H., 1949. Chemical composition and optical properties of common clinopyroxenes. Part I. Amer. Miner. 34, 621-666.

_____ 1952. Orthopyroxenes of the Bushveld type, ion substitutions, and changes in unit cell dimensions. Amer. J. Sci. Bowen Volume, 173-187.

_____ 1960. Carribean research project progress report. Geol. Soc. Amer. Bull. 71, 235-40.

_____ 1964. The oceanic crust, the upper mantle and the Mayaguez serpentinized peridotites in "A study of serpentinite". National Research Council Publication 1188.

Joplin, G.A., 1963. Chemical analyses of Australian rocks; Part I: Igneous and metamorphic. Bur. Min. Resour. Aust. Bull. 65.

Kulp, J.L., 1961. Geologic time scale. Science 133, 1105-1114.

Kuno, H., and Hess, H.H., 1953. Unit cell dimensions of clinoenstatite and pigeonite in relation to other common clinopyroxenes. Amer. J. Sci. 251, 741-752.

Lindsley, D.H., Davis, B.T.C., and Macgregor, I.D., 1964. Ferrosilite ($FeSiO_3$): synthesis at high pressures and temperatures. Science 144, 73-74.

Sarver, J.F., and Hummel, F.A., 1962. Stability relations of magnesium metasilicate polymorphs. J. Amer. Ceram. Soc. 45, 152-6.

Solar, C.B., Carrison, L.C., and Schwartz, C.M., 1964. High pressure stability field of clinoenstatite and the orthoenstatite - clinoenstatite transition. Trans. Amer. Geophys. Union 45, 121 (Abst.).

Smith, J.W., and Green, D.H., 1961. The geology of the Musa River area, Papua. Bur. Min. Resour. Aust. Rep. 52.

Stanley, E.R., 1916. Report on the geology of the Cape Vogel peninsula. Mines Dept. Rept., Territory of Papua. (unpublished).

Taylor, G.A., 1958. The 1951 eruption of Mt. Lamington, Papua. Bur. Min. Resour. Aust. Bull. 38.

Thompson, J.E., 1957. The Papuan Ultrabasic Belt. Bur. Min. Resour. Aust. Record 1957/77. (unpublished).

Tilley, C.E., Yoder, H.S., and Schairer, J.F., 1964. New relations on melting of basalts. Carnegie Inst., Washington, Year Bk. 63, 92-97.

Turner, F.J., 1942. The determination of extinction angles in monoclinic pyroxenes and amphiboles. Amer. J. Sci. 240, 571-583.

_____, Heard, H., and Griggs, D.T., 1960. Experimental deformation of enstatite and accompanying inversion to clinoenstatite. Rept. XXIst Session Internat. Geol. Congr. Copenhagen, pt. xviii, 399-408.

_____, and Verhoogen, J., 1960. Igneous and metamorphic petrology. New York: McGraw-Hill Book Company, Inc..

LEGENDS TO TEXT FIGURES

Fig. 1. The Papuan Basic Belt and associated volcanic rocks, North-Eastern Papua.

Fig. 2. Locality map and local geology, Cape Vogel, North-Eastern Papua.

Fig. 3. Sketches of composite crystals of bronzite and clinoenstatite (shaded). Some of the feathery terminations in longitudinal sections are green.

Fig. 4. Optical orientation of clinoenstatite. OAP: optic axial plane. Y_1, Y_2: acute bisectrices in alternating sets of twin lamellae.

Fig. 5. Ca:Mg:Fe diagram showing the composition fields of multiply twinned clinoenstatite and clear, untwinned orthopyroxene (bronzite).

Fig. 6. Compositional zoning in the bronzite phenocryst (Table 8, No.1) and associated (?)clinoenstatite rim and included clinoenstatite grain (Table 9, No.3).

Fig. 7. Marginal zoning in a clinoenstatite phenocryst.

Fig. 8. Ca:Mg:Fe diagram showing compositional variation at the margins of phenocrysts.

Fig. 9. Hypothetical phase diagram (cf. Boyd and Schairer, 1964, p.308) for natural Ca-poor pyroxenes from natural volcanic rocks. A liquidus curve for the Cape Vogel rock is drawn in a position compatible with the observed sequence of pyroxene crystallization.

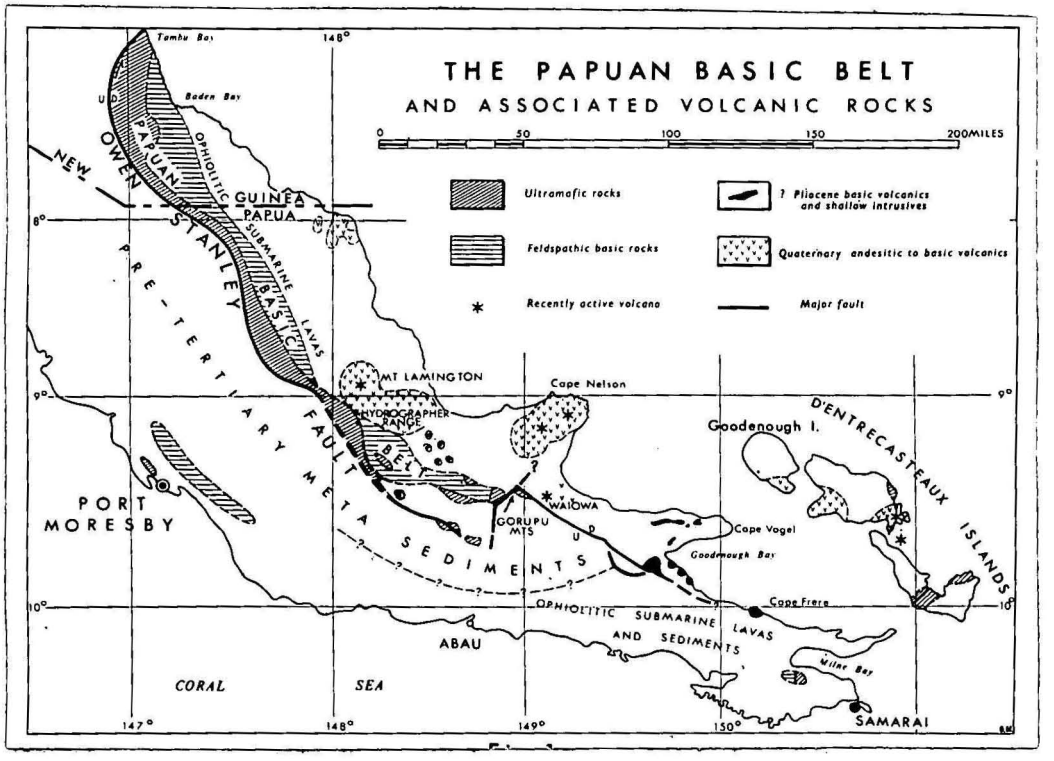
THE PAPUAN BASIC BELT
AND ASSOCIATED VOLCANIC ROCKS
0 50 100 150 200 MILES
Ultramafic rocks
Feldspathic basic rocks
Recently active volcano
? Pliocene basic volcanics and shallow intrusives
Quaternary andesitic to basic volcanics
Major fault
Tambu Bay
Baden Bay
148°
8°
9°
10°
147°
149°
150°
NEW GUINEA
PAPUA
OWEN STANLEY
PAPUAN ULTRAMAFIC BELT
OPHIOLITIC SUBMARINE BASIC LAVAS
PRE-TERTIARY META SEDIMENTS
FAULT
MT LAMINGTON
HYDROGRAPHER RANGE
Cape Nelson
Goodenough I.
D'ENTRECASTEAUX ISLANDS
PORT MORESBY
GORUPU MTS
WAIOWA
Cape Vogel
Goodenough Bay
Cape Frere
OPHIOLITIC SUBMARINE LAVAS AND SEDIMENTS
ABAU
Milne Bay
CORAL SEA
SAMARAI

Fig. 1

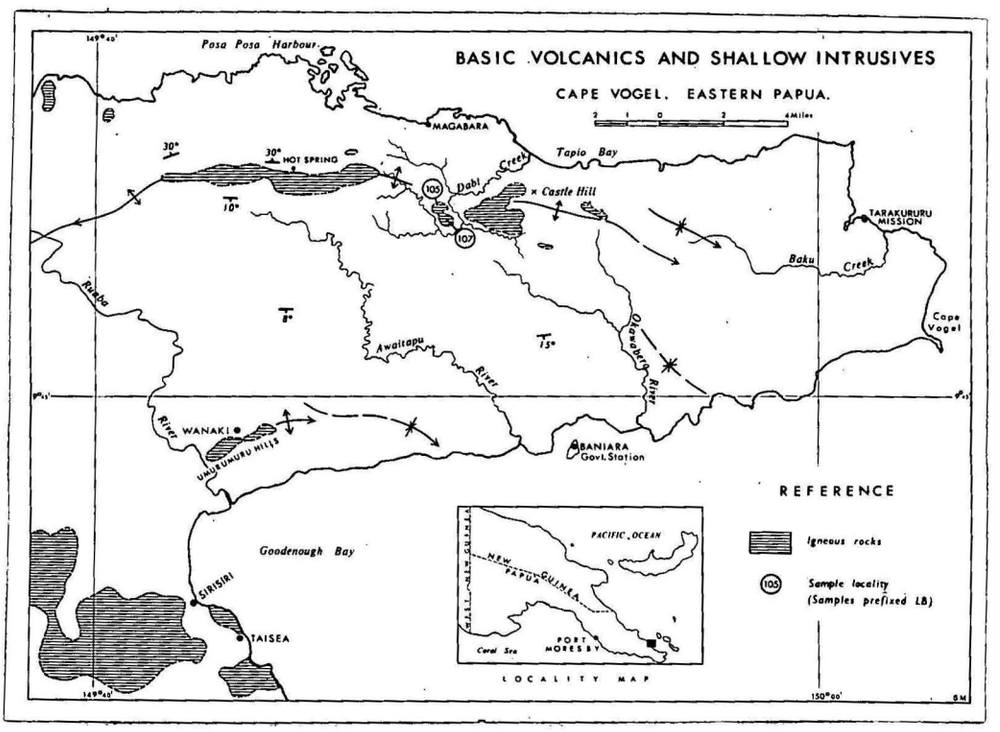
BASIC VOLCANICS AND SHALLOW INTRUSIVES
CAPE VOGEL. EASTERN PAPUA.
2 1 0 2 4 Miles
Port Moresby
MAGABARA
HOT SPRING
Tapio Bay
Dabi Creek
Castle Hill
TARAKURURU MISSION
Baku Creek
Cape Vogel
Awaitapu River
Orodubo River
WANAKI
UMUKUMURU HILLS
ABANIARA Govt. Station
Goodenough Bay
SIRISIRI
TAISEA
REFERENCE
Igneous rocks
Sample locality (Samples prefixed LB)
PACIFIC OCEAN
NEW PAPUA GUINEA
Coral Sea
PORT MORESBY
LOCALITY MAP
149°40'
150°00'
8M

Fig. 2

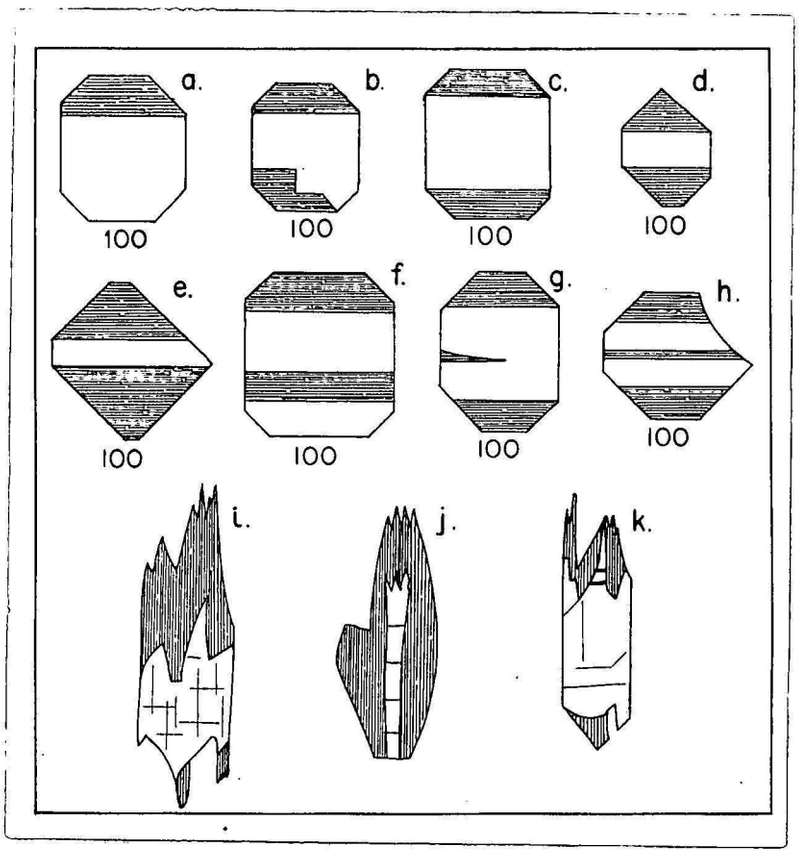

Fig. 3.

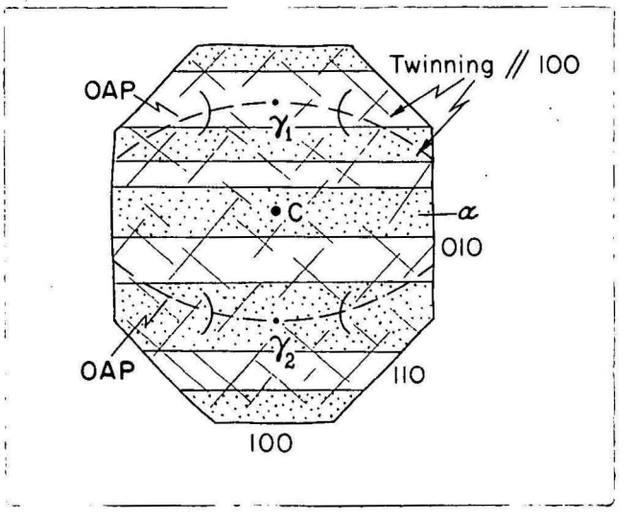

Fig 4

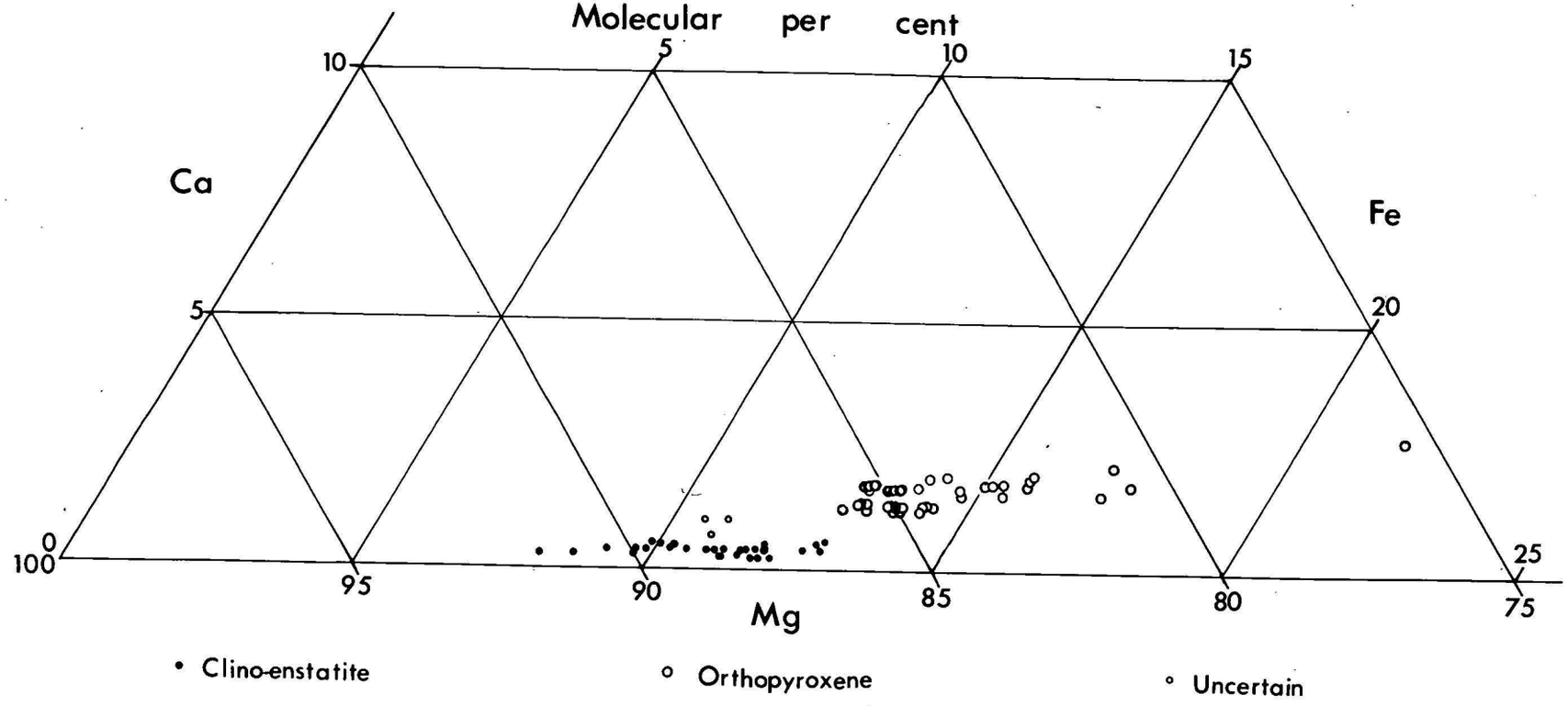
Molecular per cent
Ca
Fe
Mg
10
5
0
100
5
10
15
20
25
95
90
85
80
75
• Clino-enstatite
o Orthopyroxene
° Uncertain

Fig. 5

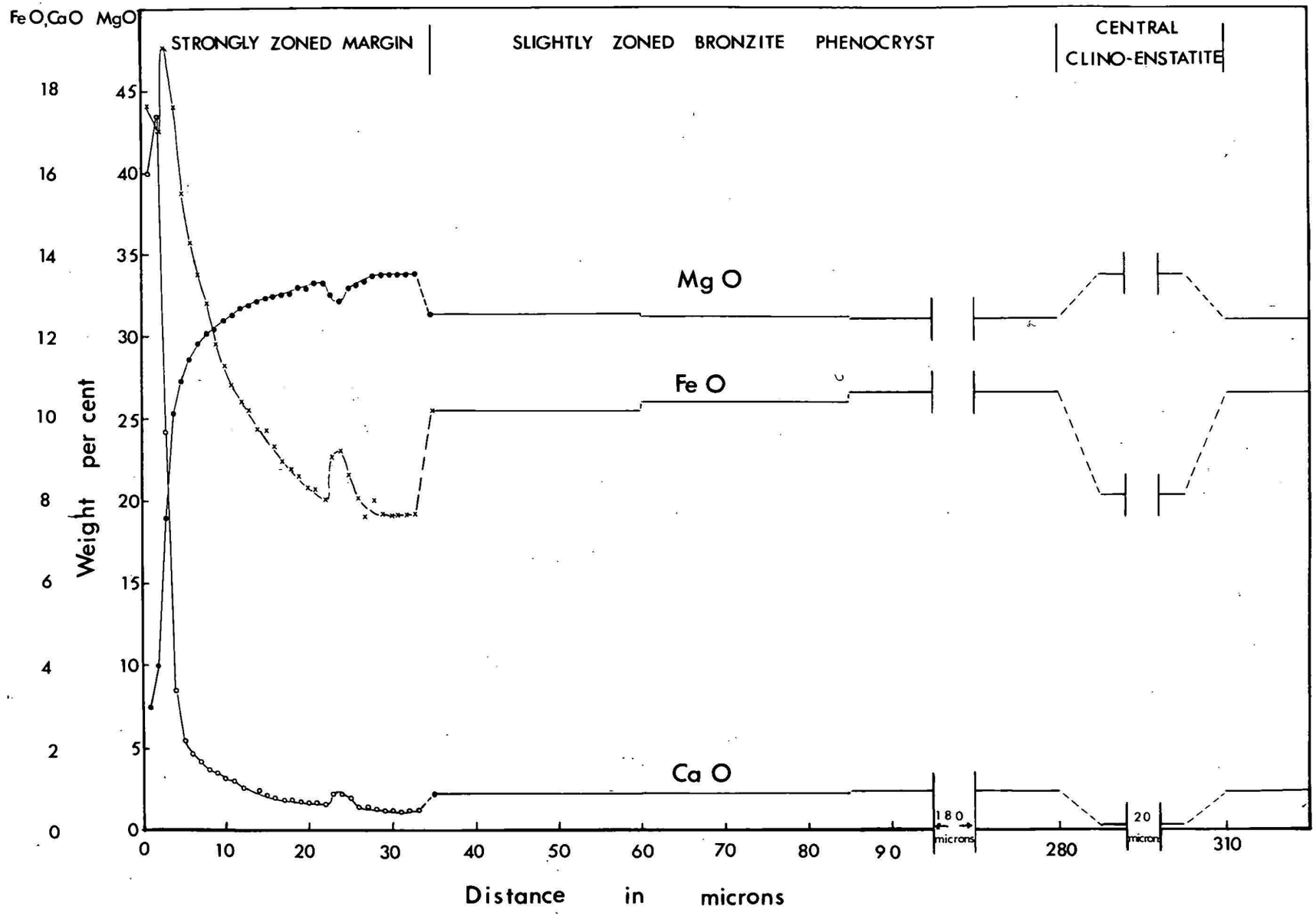
Fe O, Ca O Mg O
STRONGLY ZONED MARGIN
SLIGHTLY ZONED BRONZITE PHENOCRYST
CENTRAL
CLINO-ENSTATITE
Mg O
Fe O
Ca O
Weight per cent
Distance in microns
180 microns
20 microns
0 10 20 30 40 50 60 70 80 90 280 310
0 2 4 6 8 10 12 14 16 18
0 5 10 15 20 25 30 35 40 45

Fig. 6

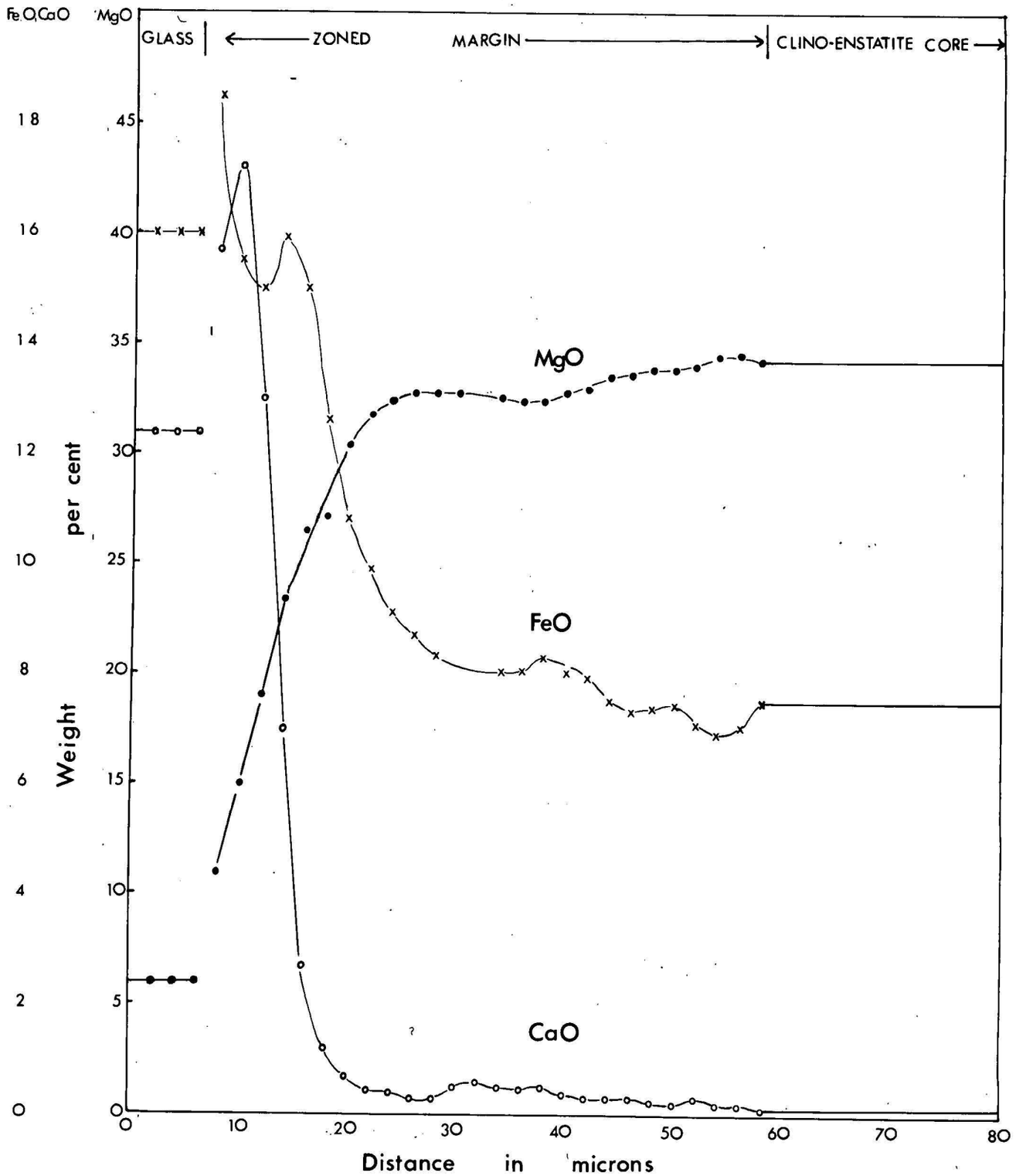
FeO,CaO
MgO
GLASS
ZONED
MARGIN
CLINO-ENSTATITE CORE
MgO
FeO
CaO
Weight per cent
Distance in microns
0
2
4
6
8
10
12
14
16
18
0
5
10
15
20
25
30
35
40
45
0
10
20
30
40
50
60
70
80

Fig. 7.

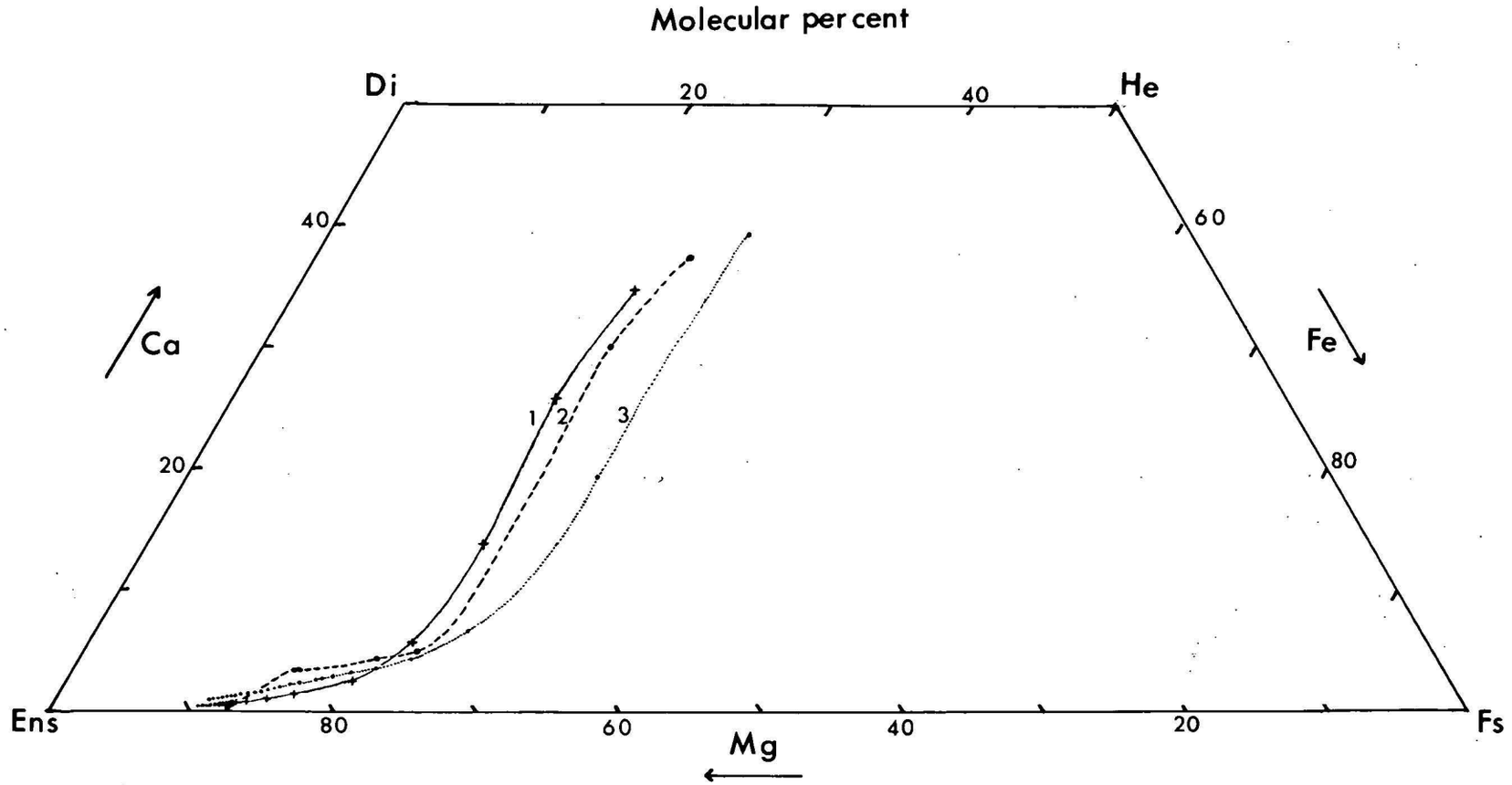

1,2. Clino-enstatite zoning 3 Orthopyroxene zoning

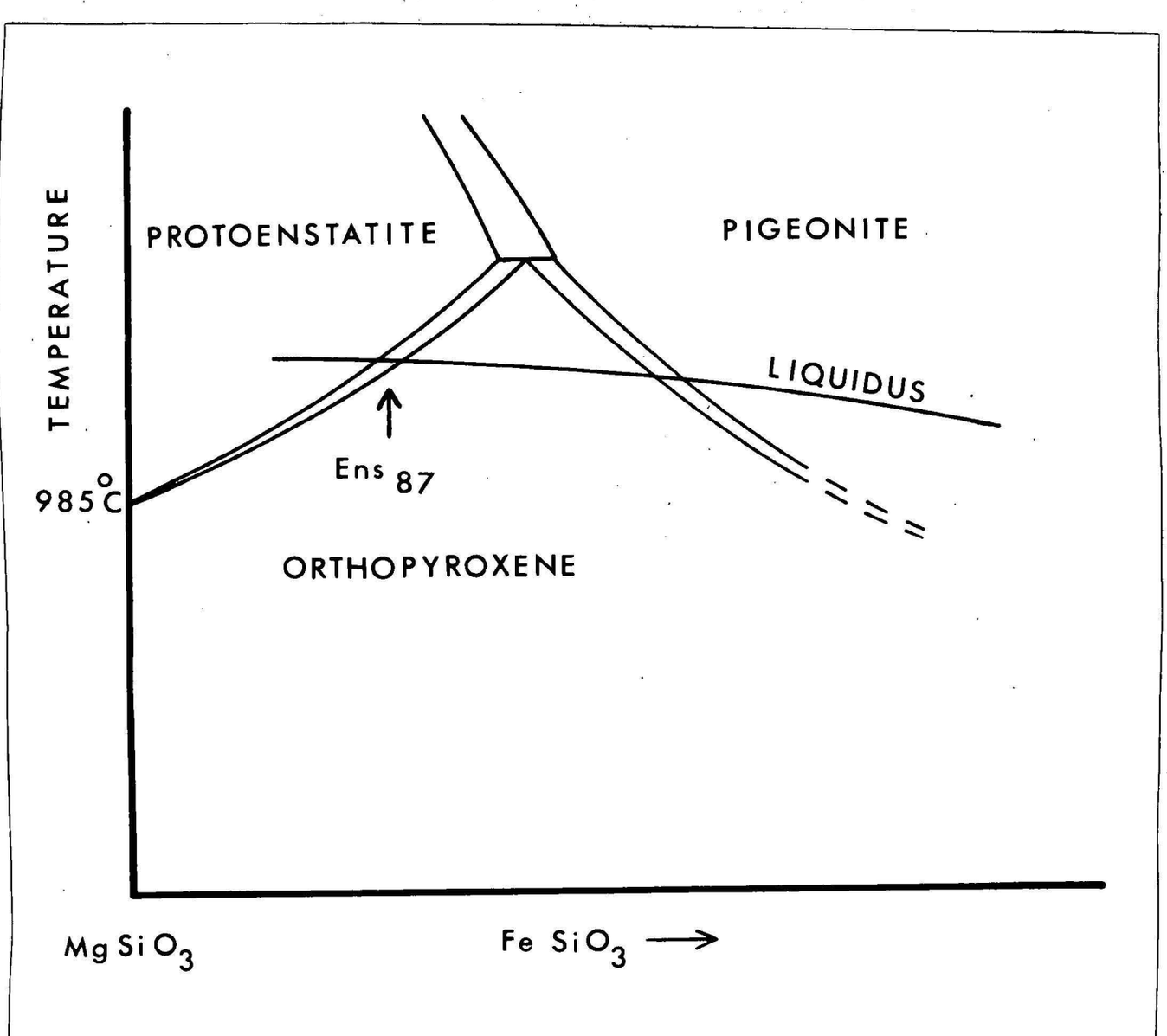
TEMPERATURE
PROTOENSTATITE
PIGEONITE
LIQUIDUS
Ens 87
985°C
ORTHOPYROXENE
Mg Si O3
Fe Si O3 →

Fig. 9.

EXPLANATION OF PLATES

PLATE 1

Fig. A. Specimen LB107, showing phenocrysts of clinoenstatite (grey), bronzite (top left), and chrome spinel in a matrix of unaltered glass (off-white), altered glass (medium to dark grey), pyroxene microlites, and zeolites (white). ×42

Fig. B. Specimen LB107. Cross section of clinoenstatite showing multiple twinning parallel to (100). Note parting parallel to (010), especially in long, white lamella. Crossed nicols. ×47

Fig. C. Specimen LB107. Longitudinal sections of contiguous euhedra of clinoenstatite with slightly different orientations. Note cleavage or parting at right angles to long axes, and strong curvature of terminal faces. Crossed nicols. ×80

Fig. D. Specimen LB107. Section of clinoenstatite cut parallel to the twin plane (100). Note prominent cleavages or partings, dark (i.e., green) border, small, wedge-shaped outgrowths of dark (green), iron-rich pyroxene, and curvature of terminal faces. ×96

PLATE 2

Fig. A. Specimen LB107. Cross section of clinoenstatite showing a rim of more iron-rich pyroxene with relatively high birefringence. The rim is about half the usual width in this crystal, whose size lies between that of the smallest

phenocryst and that of the microlites. The minute excrescences along the ($\bar{1}10$) and (010) faces of the crystal are in optical continuity with the outer zone. Crossed nicols. × 192

Fig. B. Specimen LB107. Euhedral crystal of bronzite showing four zones. Crossed nicols. × 35

Fig. C. Specimen LB107. Subhedral grain of bronzite with outgrowths of clinoenstatite. Similar relationship also figured at top right of picture, but clinoenstatite developed on one side only. Crossed nicols. × 96

Fig. D. Specimen LB107. Subhedral grain of bronzite, with outgrowths of clinoenstatite, enclosing a small grain of clinoenstatite. Crossed nicols. × 47

Fig. E. Specimen LB107. Part of large subhedral crystal of bronzite with inclusions of clinoenstatite (centre and lower left of picture). This crystal contains several more inclusions similar to the more indistinct one shown at lower left. Note also narrow, more highly birefringent rim of calcic clinopyroxene near top of picture and above scale mark. Crossed nicols. × 25

PLATE 3

Fig. A. Specimen LB107. Pyroxene microlites showing cross-fractures and dark (green) borders and feathery terminations. A cross-section (very dark) of a green microlite appears in the left centre of the photograph. Groundmass is unaltered glass (white), altered glass (grey), and a little zeolite (white with dark (altered glass) border), at bottom of picture. Note cross-fractures at right angles to c-axes of microlites. × 96

Fig. B. Specimen LB105. Longitudinal section of microlite of colourless pyroxene (grey) bordered by more highly birefringent clinopyroxene. Note cross-fractures at right angles to c-axis. Crossed nicols. ×120

Fig. C. Specimen LB107. Octagonal cross-section of composite crystal of bronzite and clinoenstatite. Crossed nicols. × 192

Fig. D. Specimen LB105. General view showing main differences from LB107 (Plate 1, fig. A). Bronzite, top right, white with (rare) clouded core; clinoenstatite phenocrysts uneven grey; elongated microlites of pyroxene; altered glass dark grey; zeolites white and off-white with altered glass (light grey) as zones and cores; unaltered glass (white), top right; typical grain of chrome spinel in bronzite. × 70

Plate 1

Figs. A to D

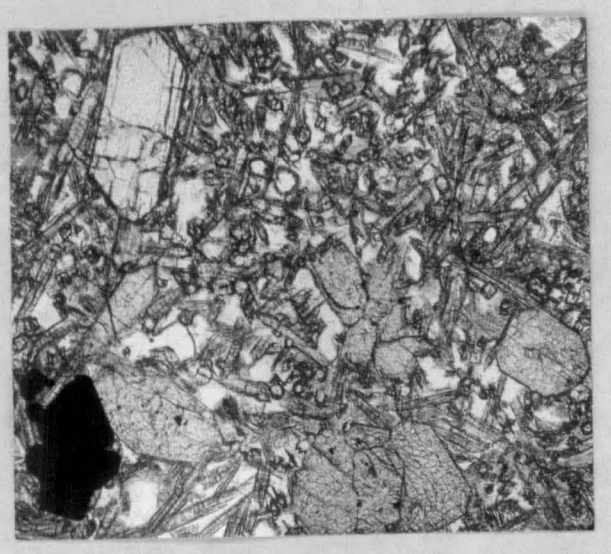

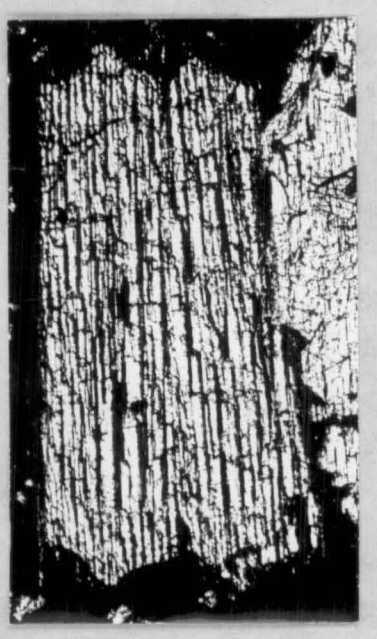

Plate 2, Figs. A to E

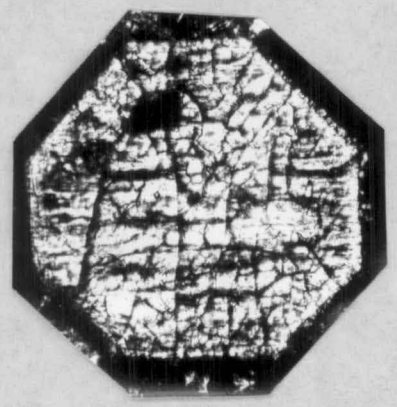

A

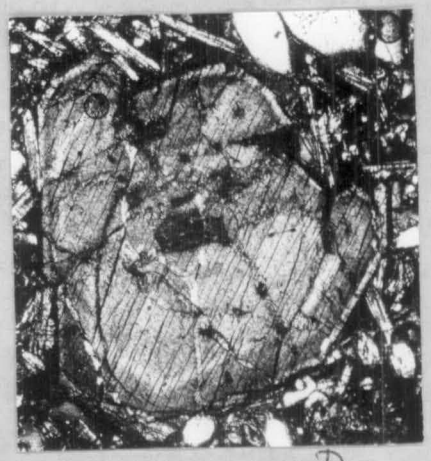

B

C

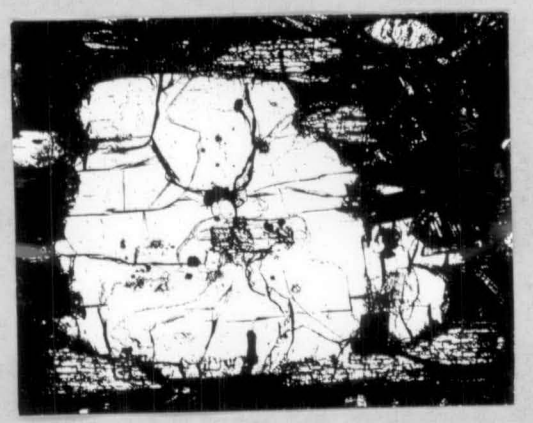

D

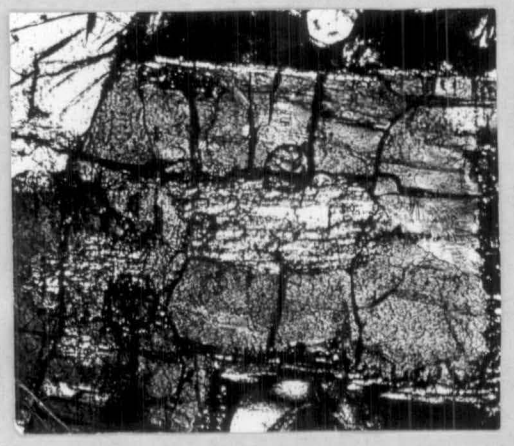

E

Plate 3

Figs. A to D

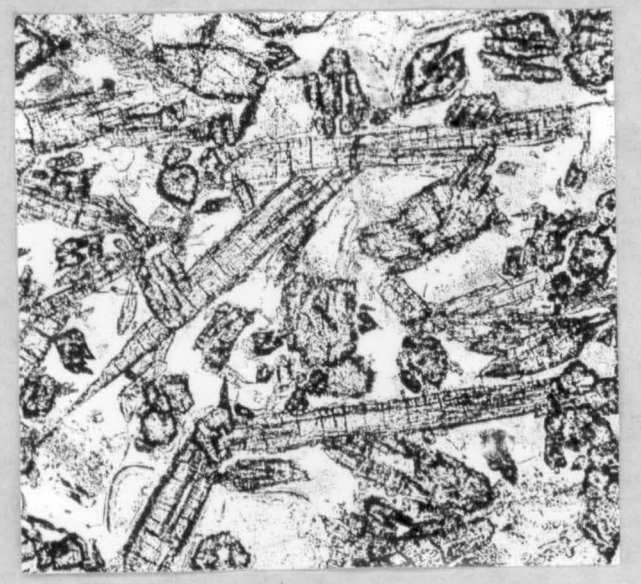

A

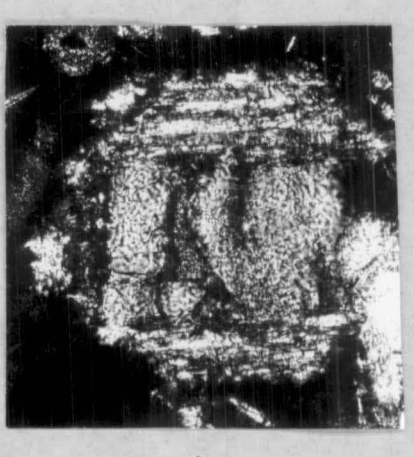

C

B

D